Transcriptomic Analysis Reveals the Contribution of *QMrl-7B* to Wheat Root Growth and Development

Jiajia Liu
Center for Agricultural Resources Research, Institute of Genetics and Developmental Biology, Chinese Academy of Sciences
Hanwen Li
College of Agronomy and Biotechnology, China Agricultural University
Na Zhang
Center for Agricultural Resources Research, Institute of Genetics and Developmental Biology, Chinese Academy of Sciences
Deyuan Meng
Center for Agricultural Resources Research, Institute of Genetics and Developmental Biology, Chinese Academy of Sciences
Liya Zhi
Center for Agricultural Resources Research, Institute of Genetics and Developmental Biology, Chinese Academy of Sciences
Xiaoli Ren
Center for Agricultural Resources Research, Institute of Genetics and Developmental Biology, Chinese Academy of Sciences
Jun Ji
Center for Agricultural Resources Research, Institute of Genetics and Developmental Biology, Chinese Academy of Sciences
Zhenqi Su
College of Agronomy and Biotechnology, China Agricultural University
Junming Li
Center for Agricultural Resources Research, Institute of Genetics and Developmental Biology, Chinese Academy of Sciences
Xiaoli Fan
Chengdu Institute of Biology, Chinese Academy of Sciences
Liqiang Song (lqsong@sjziam.ac.cn)
Center for Agricultural Resources Research, Institute of Genetics and Developmental Biology, Chinese Academy of Sciences

---

Research Article

Keywords: Triticum aestivum, Root traits, RNA sequencing, Differentially expressed gene

Posted Date: December 17th, 2020

DOI: https://doi.org/10.21203/rs.3.rs-124839/v1

Abstract

Backgound: Roots are the major organs for water and nutrient acquisition and substantially affect plant growth, development and reproduction. Improvements to root system architecture are highly important for increasing yield potential of bread wheat. *QMrl-7B*, a major stable quantitative trait locus (QTL) that controls maximum root length (MRL), strongly contributes to an improved root system in wheat.

Results: To further analyse the biological functions of *QMrl-7B* in root development, two types of *Triticum aestivum* near isogenic lines (NILs), one with superior *QMrl-7B* alleles from cultivar Kenong 9204 (KN9204) and another with inferior *QMrl-7B* alleles from cultivar Jing 411 (J411), were subjected to transcriptomic analysis. Among all the mapped genes analysed, 4871 genes were identified as being differentially expressed between the pairwise NILs under different nitrogen (N) conditions, with 3543 genes expressed under normal-nitrogen (NN) condition and 2689 genes expressed under low-nitrogen (LN) condition. These genes encode proteins that include mainly NO_3^- transporters, phytohormone signalling components and transcription factors (TFs), indicating the presence of a complex regulatory network involved in root determination. In addition, among the 13524 LN-induced differentially expressed genes (DEGs) detected in this assay, 4308 were specifically expressed in the A-NIL which brings superior alleles, and 2463 were expressed specifically in the B-NIL which brings inferior alleles. These DEGs reflect different responses of the two types of NILs to varying N supplies, which likely involve LN-induced root growth.

Conclusions: These results explain the better-developed root system and increased root vitality provided by the superior alleles of *QMrl-7B* and provide a deeper understanding of the genetic underpinnings of root traits, pointing to a valuable locus suitable for future breeding efforts for sustainable agriculture.

Background

Crops produce a large proportion of food and nutrients for humans in modern society. During the past 50 years, the application of chemical fertilizers and the Green Revolution have substantially increased crop production, maintaining food security for the increasing growing population [1–2]. However, a continuous increase in crop output cannot sustainably be achieved by excessive amounts of fertilizer because of the limited nutrient use efficiency of crop plants [3]. Importantly, a large amount of wasted resources and environmental pollution resulting from excessive fertilizer applications cannot be ignored [4]. For these reasons, crop cultivars that have relatively high nutrient use efficiency, are environmentally friendly and conserve resources are necessary for sustainable agriculture. Roots, the major organs for plant anchorage, nutrient and water absorption and interactions with symbiotic organisms, have been chronically overlooked in domestication and selection due to their lack of aboveground visibility. Fortunately, root traits, including root number, root length, root surface area (RA) and root volume (RV), have attracted increased amounts of attention in recent studies given the discovery of their correlations with nutrient use and crop yield [5–6]. In general, manipulation of root architecture traits, especially the spatial configuration of the root system in the soil, is an essential approach to increase crop yields, which may represent an important component of a new green revolution [7–8].

Bread wheat (*Triticum aestivum* L.) is one of the most important crop species worldwide, providing ~ 20% of calories for human needs (FAO stats, http://www.fao.org/faostat/). Efforts have been made to explore the determinants of root traits that contribute to increased yields in wheat. In addition to traditional labour-intensive and time-consuming methods for root trait analysis [9], artificial medium systems, such as hydroponic culture, have been used in many studies and have revealed a series of quantitative trait loci (QTLs) that drive genetic variation in

root traits [10–16]. However, the mechanisms through which these loci control root traits remain largely unclear due to the complexity of the wheat genome. Fortunately, knowledge of diploid model systems and orthologous gene analysis has provided valuable information for root research in wheat. Specifically, reverse genetics studies have resulted in the cloning of several wheat genes involved in the regulation of root morphology. For example, the expression of *TaRSL2* [17] and *TaLBD16* [18] was shown to be positively correlated with root hair length and number of lateral roots on the primary root, respectively. Heterogenous expression of *TaMPK4* [19] and *TaMOR1* [20] demonstrated their positive effects on root development. Overexpression of the transcription factor (TF)-encoding genes *TaNAC2-5A* [21], *TaNFYA-B1* [22], *TaNAC69-1* [23] and *TaWRKY51* [24] resulted in enhanced root growth, while the TF-encoding gene *TabZIP60* [25] had the opposite effects, implying a complex genetic basis of the formation of root traits. In addition, circular RNAs have been shown to participate in root length regulation [26].

At present, a holistic view of the root growth regulatory network and how it affects root traits and yield potential is strongly needed for molecular breeding. RNA sequencing (RNA-seq) makes it possible to explore the consistency between root morphology and its underlying mechanisms at the whole-plant level through differentially expressed gene (DEG) analysis. For example, transcriptomic analysis revealed how the growth of roots of salt-tolerant bermudagrass was maintained under salinity stress; the ability was attributed to appropriate expression levels of genes involved in reactive oxygen species (ROS) homeostasis and cell wall loosening, which were regulated in part by a number of TFs linked to stress responses and growth regulation [27]. DEGs detected in maize cultured under different nitrogen (N) levels highlighted the network of root growth in response to N deficiency, where the *LBD* TF-encoding gene participates in the balance between nutrient metabolism and the stress response [28]. RNA-seq data suggested crosstalk occurs among the roots (in terms of growth promotion), gibberellin (GA) biosynthesis, auxin signalling, cell division and cell wall modification in uniconazole-treated soybean [29]. These findings enriched our understanding of the molecular mechanisms behind the interplay of root traits and other agronomic characteristics, helping to generate strategies for crops with improved root systems, increased nutrient-use efficiency and improved environmental adaption.

Previous studies have shown that *Triticum aestivum* cv. Kenong 9204 (KN9204) has a larger root system than does cultivar Jing 411 (J411) [30]. Using KJ-RIL, researchers identified *QMrl-7B* as a major sable QTL that controls maximum root length (MRL) [15], and its contribution to large root systems was dissected (Liu et al., Frontiers Plant Sci, in revision), prompting the question of how it regulates root architecture. In the present study, transcriptomic analysis of pairwise *QMrl-7B* near isogenic lines (NILs) was performed to further analyse the function of *QMrl-7B* in root development. The results will help reveal the pathways controlling root development that are affected by *QMrl-7B* in wheat, providing insights into the genetic and physiologic basis underlying desirable root traits for agriculture.

Results

Root traits of the pairwise NILs

The root traits of the seedlings in hydroponic cultures with different N contents were evaluated. On the fourteenth day after the seedlings were transferred to the nutrient solutions, the average MRL, TRL, RA and RV of the four-leaf-stage A-NIL seedlings were 22.28 cm, 255.77 cm, 25.47 cm^2 and 0.25 cm^3, respectively, under NN condition, which were significantly greater than those of the B-NIL (19.85 cm, 203.47 cm, 20.64 cm^2 and 0.20 cm^3, respectively) under comparable conditions. Accordingly, the average MRL, TRL, RA and RV of the A-NIL vs B-NIL at the seedling stage were 28.07 vs 21.54 cm, 301.75 vs 282.12 cm, 27.28 vs 24.90 cm^2 and 0.25 vs 0.21 cm^3, respectively, under LN condition, indicating that the A-NIL were superior to the B-NIL by 30.32%, 6.96%, 9.56% and 19.05%, respectively

($p < 0.05$). Notably, the MRL of the A-NIL seedlings under LN condition was 25.99% greater than that under NN conditions, while only an 8.51% difference was recorded for the B-NIL under the hydroponic cultures with different N contents, indicating that LN more strongly induced the growth of primary roots for the A-NIL than for the B-NIL (Figure 1). Similar change trends of MRL, TRL, RA and RV differences in the five-leaf-stage seedlings were also observed between the two types of NILs at 21 days after the 10-day-old seedlings were transferred (with their endosperm removed) to the nutrient solutions (Figure S1). Taken together, the above results showed that, as compared to the B-NIL, the A-NIL had superior root architecture characteristics during the seedling stage, especially under LN condition.

Overview of transcriptome sequencing results

To explore the genetic and physiologic basis of the superior root traits of the A-NIL, roots of four-leaf-stage seedlings of the pairwise NILs cultured under both NN conditions and LN conditions were sampled for transcriptomic analysis. RNA-seq on the Illumina HiSeq^{TM} platform (http://www.majorbio.com) generated 70576620~90524786 clean reads per sample, with a sequencing error less than 0.3%. The average Q20, Q30 and GC content percentages were 97.06%, 92.27% and 53.98%, respectively. These findings attest to the fine quality of the sequencing results. Mapping of the reads with the CS reference genome revealed an alignment in a range of 81.48~90.35%, among which 76.14~84.54% of the genes were uniquely mapped and of which 5.34~6.28% were multiply mapped (Table S2). The correlation coefficient of repeats ranged from 0.69~0.98 (Figure S2, Table S3). These data were deemed suitable for subsequent analysis (Table S4), in which the DEGs whose expression was upregulated ($\log_2FC \geq 1$) and downregulated ($\log_2FC \leq -1$) in each one-to-one comparison were statistically (p-adjusted < 0.05) analysed.

Identification of DEGs between the pairwise NILs

The transcriptomic changes in the roots between the pairwise *QMrl-7B* NILs were compared under both NN and LN conditions. Under NN condition, a total of 3543 genes were differentially expressed between the two types of NILs, of which the expression of 1045 genes was upregulated and that of 2498 was downregulated in the A-NIL (Figure 2A, Table S5). These genes were enriched in 320 subcategories according to GO analysis, of which 200, 14 and 106 belong to biological processes, cellular components and molecular functions, respectively, and the 3 most enriched biological processes were “biological process (GO:0008150)”, “metabolic process (GO:0008152)” and “phosphate-containing compound metabolic process (GO:0006796)” (Table S6). “Phenylpropanoid biosynthesis (map00940)” was the most enriched pathway according to KEGG analysis (Table S7). Under LN condition, 2689 genes were differentially expressed between the pairwise NILs, including 990 genes whose expression was upregulated and 1699 whose expression was downregulated in the A-NIL (Figure 2A, Table S8). These DEGs were categorized into biological process (141), cellular component (12) and molecular function (77) categories by GO analysis. The 3 most enriched biological processes were “biological process (GO:0008150)”, “metabolic process (GO:0008152)” and “phosphate-containing compound metabolic process (GO:0006796)” (Table S9). Similarly, “phenylpropanoid biosynthesis (map00940)” was the most enriched pathway according to the KEGG analysis (Table S10).

Notably, there were 315 DEGs whose expression increased and 1034 DEGs whose expression decreased in the A-NIL compared to the B-NIL simultaneously under both NN and LN conditions (Figure 2A). These genes might participate in translation, transcriptional regulation and cycle control according to GO and KEGG enrichment analysis (Figure 2B, Tables S11-S13), reflecting the permanent effects of the *QMrl-7B* locus that were not affected by N levels. Under NN condition, 9 genes were expressed at higher levels in the A-NIL than in the B-NIL; however, these genes were

expressed at a higher level in the B-NIL under LN condition (Figure 2A, Table 1). In addition, 3 genes exhibited the opposite expression trend, implying their functional difference in response to N stress (Figure 2A, Table 1).

Table 1
DEGs with opposite expression patterns between the pairwise NILs under NN and LN conditions

Gene_id	log_2FC (NN_AA/NN_BB)	*p*-adjusted	log_2FC (LN_AA/LN_BB)	*p*-adjusted	NR_description
TraesCS2A02G399900	1.07	0.002	-1.97	7.77E-20	MATE efflux family protein 9
TraesCS2B02G125500	-1.37	0.0098	1.08	1.25E-06	class III peroxidase
TraesCS2B02G626400	-5.11	2.88E-34	1.11	2.48E-05	probable 1-deoxy-D-xylulose-5-phosphate synthase 2, chloroplastic
TraesCS3B02G448000	1.74	1.07E-18	-1.35	1.98E-06	unnamed protein product
TraesCS3D02G094500	-2.06	5.54E-07	1.68	0.001	MYB-related protein 305-like
TraesCS3D02G225500	1.16	0.0002	-1.42	4.08E-14	uncharacterized protein LOC109770081
TraesCS3D02G408000	1.21	2.62E-07	-1.68	4.76E-16	BTB/POZ and TAZ domain-containing protein 2-like
TraesCS4A02G286600	1.32	4.98E-05	-1.73	2.50E-10	uncharacterized protein LOC109755115
TraesCS4B02G078800	1.85	3.67E-15	-1.07	5.58E-06	hypothetical protein TRIUR3_28321
TraesCS4D02G025500	1.18	0.0003	-1.97	2.85E-08	uncharacterized protein LOC109755115
TraesCS6B02G044300	1.15	0.001	-1.47	4.78E-08	high-affinity nitrate transporter TaNRT2
TraesCS6D02G035900	1.01	0.016	-1.02	0.002	high-affinity nitrate transporter 2.1-like

NN and LN indicate normal- and low-nitrogen conditions, respectively. AA and BB indicate the A-NIL and the B-NIL, respectively. The expression levels between the A-NIL and the B-NIL were compared under each condition, with the latter as a control. The expression ratios are presented as log_2FC values. Genes with a $log_2FC \leq -1$ (*p*-adjusted < 0.05, coloured blue) represent the genes whose expression was downregulated in the A-NIL, and genes with $log_2FC \geq 1$ (*p*-adjusted < 0.05, coloured red) represent the genes whose expression was upregulated in the A-NIL.

Identification of DEGs in response to N deficiency

The differences in DEGs in the root response to N deficiency between the A-NIL and B-NIL were analysed. Compared with the NN condition, LN condition yielded 11073 DEGs (6341 whose expression increased and 4732 whose expression decreased) and 9228 DEGs (5072 whose expression increased and 4156 whose expression decreased) in the A-NIL and B-NIL, respectively (Figure 3A). A total of 2385 DEGs whose expression increased and 1923 DEGs whose expression decreased were detected only in the A-NIL (Figure 3A, Table S14), whereas 1116 DEGs whose expression increased and 1347 DEGs whose expression decreased were detected specifically in the B-NIL (Figure 3A, Table S17). Interestingly, there were more genes whose expression was upregulated than genes whose expression was downregulated in the A-NIL, and the opposite trend occurred in the B-NIL. GO analysis showed that these DEGs participate in multiple processes, and “phenylpropanoid biosynthesis (map00940)” was the most enriched process according to KEGG analysis (Figure 3B and 3C, Tables S14-S19). The expression of genes that differed specifically in the A-NIL or the B-NIL might give rise to a specific N response related to *QMrl-7B*, while the large number of common DEGs (3956 genes whose expression was upregulated and 2809 genes whose expression downregulated) in the two types of NILs reflected the general response to N stress in wheat.

Real-Time PCR (qPCR) verification

qPCR analysis revealed that the expression levels of eight randomly selected DEGs on chromosome 7B were significantly different between the A-NIL and the B-NIL under NN conditions and LN conditions (Figure 4). These results nearly matched the expression profiles revealed by RNA sequencing, confirming the results of the transcriptome sequencing of the pairwise NILs cultured under both NN and LN conditions.

Discussion

Improving plant roots is an effective way to increase nutrient use efficiency and minimize fertilizer application for sustainable agricultural development. A number of genes/QTLs have been reported to be related to root growth and development; as such, these genes/QTLs have potential application for use in crop genetic improvement. However, the genetic network explaining how these genes interact to influence root architecture still needs to elucidated to assess the beneficial agronomic traits from an overall perspective and to guide the use of beneficial genes or pyramiding of allelic variation in future breeding efforts. Compared with J411, KN9204 has a larger root system, with which the stable QTL *QMrl-7B* is associated [15, 30]. Further studies involving *QMrl-7B* NILs showed that, as compare to the B-NILs, the A-NILs had superior root traits, N-related traits and yield traits in field trials (Liu et al., Frontiers Plant Sci, in revision). The superiority of root traits of the A-NIL at the seedling stage was also consistently proven in the present study. When these hydroponically cultured pairwise NILs were used for transcriptomic analysis, it was found that the DEGs detected by RNA-seq encode proteins of various groups, such as transporters, enzymes, TFs, and components involved in hormone signalling. The important DEGs that might be involved in root trait regulation are discussed here.

The genes with opposite expression patterns between the pairwise NILs under the NN and LN conditions are very likely to be involved in N-related root growth (Tables 1, S5 and S8). For example, the expression level of the class III peroxidase gene (TraesCS2B02G125500) was higher in the B-NIL under NN condition but was higher in the A-NIL under LN condition. Class III peroxidase uses H_2O_2 as a substrate to produce OH^- radicals that enhance cell wall plastic extensibility and elongation by nonenzymatic cleavage of cell wall polysaccharides [31–33]. Because root development is directly related to cell wall loosening and elongation [34], the upregulated expression of this gene by LN in the A-NIL (Table S14) may participate in LN-promoted root growth by affecting these processes. Since the most enriched process of the DEGs between the pairwise NILs is phenylpropanoid biosynthesis, the relation of

phenylpropanoid and root traits is worthy of attention. Phenylpropanoids are a source of many secondary metabolites, such as lignin, coumarin and flavonoids. Phenylalanine ammonia-lyase and cinnamoyl-CoA reductase catalyse the biosynthesis of cinnamate and lignin monomers, which are important metabolites in phenylpropanoid metabolism [35]. It was found that enhanced phenylpropanoid biosynthesis promotes root growth in rice [36], implying that there are positive effects of this metabolite on plant growth, including root enlargement [37]. Interestingly, the expression levels of a series of phenylalanine ammonia-lyase and cinnamoyl-CoA reductase genes increased in the B-NIL under both NN and LN conditions (Tables S5 and S8), implying that the biosynthesis of cinnamate and lignin monomers increased, which cannot directly explain the reason for the smaller roots.

Low-affinity NO_3^- transporters and high-affinity NO_3^- transporters work under conditions of different N levels; the latter specifically transports NO_3^- and thus is more likely to reflect a response to N stress [38]. Dual-affinity nitrate transporter 1 (NRT1) not only functions in N acquisition but also is a NO_3^- sensor; this action is independent of its uptake activity that controls root development [39–41]. The cotransport of NO_3^-, peptides and hormones through the NRT1 family of transporters implies the occurrence of crosstalk between NO_3^- and other signalling pathways [42–44]. In addition, N stress tolerant genotypes exhibit higher expression levels of high-affinity NRTs than do the sensitive genotypes under N-limiting conditions [45]. Among these NRTs, NRT2.1 coordinates root development with external NO_3^- availability directly through stimulation of lateral root initiation under N-limiting conditions and indirectly through its NO_3^- transport function, which affects the N-dependent root system [40]. Our results showed that LN led to altered expression of a number of genes encoding both low-affinity and high-affinity NRTs, in accordance with the viewpoint that different NRTs function at different N levels (Table S4). Among these genes, the expression levels of 2 and 11 putative NRT1 genes in the A-NIL were higher and lower than those in the B-NIL under both NN and LN conditions (Table 2), indicating that the differences in root traits may originated mainly from NRT1 functional differentiation. Additionally, the higher expression level of the CBL-interacting protein kinase 23 (CIPK23) gene (TraesCS2A02G251800) in the B-NIL compared with the A-NIL was also independent of N status (Tables S5 and S8); this phenomenon may affect root formation together with NRT1 by phosphorylating T101 to regulate its primary NO_3^- response and high-affinity NO_3^- transport [41]. Contrastingly, the expression of 4 high-affinity NRT genes (TraesCS6A02G031000, TraesCS6A02G031100, TraesCS6B02G044100 and TraesCS6B02G044500) was induced specifically by LN in the B-NIL but not in the A-NIL (Table 3). In addition, 2 high-affinity NRT genes (TraesCS6B02G044300 and TraesCS6D02G035900) exhibited higher expression levels in the B-NIL than in the A-NIL under LN condition, although under NN condition, their expression levels in the B-NIL were lower (Table 1). Taken together, these results implied that a more sensitive response of roots to N acquisition occurred in the B-NIL compared with the A-NIL, which cannot be fully explained.

Table 2
Differentially expressed *NRT* genes between the pairwise NILs

Gene_id	log_2FC (NN_AA/NN_BB)	*p*-adjusted	log_2FC (LN_AA/LN_BB)	*p*-adjusted	NR_description
TraesCS2A02G309100	-1.43	9.78E-12	-1.24	2.60E-12	protein NRT1/ PTR FAMILY 4.3-like
TraesCS2A02G572200	1.13	0.04	1.20	0.003	protein NRT1/ PTR FAMILY 5.10-like
TraesCS5A02G485200	-1.03	0.006	-1.12	0.01	protein NRT1/ PTR FAMILY 5.6-like
TraesCS5D02G498700	-2.07	4.20E-15	-2.15	1.62E-11	protein NRT1/ PTR FAMILY 5.6-like
TraesCS6A02G267600	-1.44	0.0001	-1.92	0.002	protein NRT1/ PTR FAMILY 8.3-like
TraesCS6A02G267700	-3.00	1.90E-24	-1.56	6.45E-06	protein NRT1/ PTR FAMILY 8.3-like
TraesCS6A02G267800	-3.23	3.26E-05	-2.90	0.006	protein NRT1/ PTR FAMILY 8.3-like
TraesCS6A02G268500	-1.09	7.42E-05	-1.56	0.005	protein NRT1/ PTR FAMILY 8.3-like
TraesCS6B02G295000	-2.41	1.52E-13	-2.40	5.56E-08	protein NRT1/ PTR FAMILY 8.3-like
TraesCS6B02G295600	-1.85	1.83E-12	-1.78	0.005	protein NRT1/ PTR FAMILY 8.3-like
TraesCS6D02G247000	-4.10	4.91E-25	-2.03	0.0001	protein NRT1/ PTR FAMILY 8.3-like
TraesCS6D02G247100	-1.45	9.32E-05	-1.88	5.83E-05	protein NRT1/ PTR FAMILY 8.3-like isoform X1
TraesCS7D02G378300	1.53	0.0004	1.04	0.008	protein NRT1/ PTR FAMILY 8.3-like isoform X1

NN and LN indicate normal- and low-nitrogen conditions, respectively. AA and BB indicate the A-NIL and the B-NIL, respectively. The expression levels between the A-NIL and the B-NIL were compared under each condition, with the latter as a control. The expression ratios are presented as log_2FC values. Genes with a $log_2FC \leq -1$ (*p*-adjusted < 0.05, coloured blue) represent the genes whose expression was downregulated in the A-NIL, and genes with $log_2FC \geq 1$ (*p*-adjusted < 0.05, coloured red) represent the genes whose expression was upregulated in the A-NIL.

Table 3

NRT genes specifically expressed in the A-NIL or B-NIL in response to LN

Gene_id	log_2FC (LN_AA/NN_AA)	*p*-adjusted	log_2FC (LN_BB/NN_BB)	*p*-adjusted	NR_description
TraesCS1A02G150200	1.03	0.004	0.14	0.84	Peptide transporter PTR3-A
TraesCS1A02G150400	1.18	2.29E-07	0.64	0.08	protein NRT1/ PTR FAMILY 5.2-like
TraesCS1B02G168100	1.60	1.11E-12	0.90	0.01	protein NRT1/ PTR FAMILY 5.2-like
TraesCS1B02G225000	-1.39	2.12E-06	-0.14	0.81	protein NRT1/ PTR FAMILY 6.3-like
TraesCS1B02G267900	1.29	0.01	1.15	0.18	protein NRT1/ PTR FAMILY 3.1-like
TraesCS1D02G201100	1.13	2.34E-11	0.81	0.0004	uncharacterized protein LOC109744571
TraesCS1D02G214300	-1.47	7.24E-08	0.20	0.72	protein NRT1/ PTR FAMILY 6.3-like
TraesCS2A02G007500	0.60	0.08	1.05	1.54E-09	protein NRT1/ PTR FAMILY 8.5-like
TraesCS2A02G074800	-1.89	0.003	-0.58	0.45	high-affinity nitrate transporter 2.1-like
TraesCS2A02G264500	0.99	8.86E-05	1.06	0.0006	protein NRT1/ PTR FAMILY 4.5-like
TraesCS2B02G277600	0.71	0.003	1.27	6.40E-09	protein NRT1/ PTR FAMILY 4.5-like
TraesCS2B02G626000	1.02	1.30E-05	0.43	0.19	protein NRT1/ PTR FAMILY 5.10-like
TraesCS2B02G626700	1.76	1.07E-08	0.97	0.01	protein NRT1/ PTR FAMILY 5.10-like
TraesCS2D02G413900	1.50	0.02	1.74	0.08	protein NRT1/ PTR FAMILY 8.2-like
TraesCS2D02G583500	0.99	0.01	1.30	0.0005	protein NRT1/ PTR FAMILY 5.10-like
TraesCS3A02G382100	-2.55	6.06E-20	-0.94	0.34	protein NRT1/ PTR FAMILY 5.1-like isoform X1

NN and LN indicate normal- and low-nitrogen conditions, respectively. AA and BB indicate the A-NIL and the B-NIL, respectively. The expression levels between the A-NIL and the B-NIL were compared under each condition, with the latter as a control. The expression ratios are presented as log_2FC values. Genes with a $log_2FC \leq -1$ (*p*-adjusted < 0.05, coloured blue) represent the genes whose expression was downregulated under LN conditions, and genes with $log_2FC \geq 1$ (*p*-adjusted < 0.05, coloured red) represent the genes whose expression was upregulated under LN conditions.

Gene_id	log_2FC (LN_AA/NN_AA)	*p*-adjusted	log_2FC (LN_BB/NN_BB)	*p*-adjusted	NR_description
TraesCS3A02G382200	-0.12	0.90	1.57	0.003	unnamed protein product
TraesCS3B02G095900	0.20	0.62	1.12	0.02	unnamed protein product
TraesCS3B02G414900	-3.35	5.34E-07	0.20	0.90	unnamed protein product
TraesCS3B02G415700	0.81	0.12	1.01	0.02	predicted protein
TraesCS3D02G056700	0.85	0.25	1.43	0.048	protein NRT1/ PTR FAMILY 8.2-like isoform X1
TraesCS4A02G225400	-1.07	6.53E-06	-0.97	0.007	protein NRT1/ PTR FAMILY 4.3-like
TraesCS4A02G283900	1.20	6.27E-15	0.93	9.83E-06	protein NRT1/ PTR FAMILY 2.11-like
TraesCS4D02G026800	1.01	1.57E-08	0.85	1.76E-05	protein NRT1/ PTR FAMILY 2.11-like
TraesCS4D02G087900	-1.39	2.77E-07	-0.997	0.002	protein NRT1/ PTR FAMILY 4.3-like
TraesCS5B02G039100	3.41	0.02	2.02	0.22	protein NRT1/ PTR FAMILY 2.11-like
TraesCS5B02G152000	1.42	0.31	3.72	0.04	putative nitrate excretion transporter 3
TraesCS5B02G245300	2.48	8.76E-05	1.89	0.09	predicted protein
TraesCS5B02G393100	1.46	0.39	4.38	0.03	protein NRT1/ PTR FAMILY 4.5-like
TraesCS5B02G414000	0.79	0.008	1.14	2.22E-05	protein NRT1/ PTR FAMILY 6.4 isoform X2
TraesCS5B02G498700	-0.82	0.02	-1.09	0.01	protein NRT1/ PTR FAMILY 5.6-like
TraesCS5D02G419200	0.89	0.03	1.91	0.0007	protein NRT1/ PTR FAMILY 6.4 isoform X1
TraesCS5D02G498700	-1.03	0.009	-0.95	0.0004	protein NRT1/ PTR FAMILY 5.6-like

NN and LN indicate normal- and low-nitrogen conditions, respectively. AA and BB indicate the A-NIL and the B-NIL, respectively. The expression levels between the A-NIL and the B-NIL were compared under each condition, with the latter as a control. The expression ratios are presented as log_2FC values. Genes with a $log_2FC \leq -1$ (*p*-adjusted < 0.05, coloured blue) represent the genes whose expression was downregulated under LN conditions, and genes with $log_2FC \geq 1$ (*p*-adjusted < 0.05, coloured red) represent the genes whose expression was upregulated under LN conditions.

Gene_id	log_2FC (LN_AA/NN_AA)	*p*-adjusted	log_2FC (LN_BB/NN_BB)	*p*-adjusted	NR_description
TraesCS6A02G030700	-2.93	7.26E-18	-0.63	0.17	high-affinity nitrate transporter 2.1-like
TraesCS6A02G030800	-2.84	1.38E-27	-0.38	0.50	high-affinity nitrate transporter 2.1-like
TraesCS6A02G030900	-2.75	1.36E-29	-0.43	0.33	High-affinity nitrate transporter 2.1
TraesCS6A02G031000	0.20	0.78	1.63	0.0002	High-affinity nitrate transporter 2.1
TraesCS6A02G031100	0.01	0.98	1.45	3.00E-05	high affinity nitrate transporter
TraesCS6A02G033100	-6.88	4.09E-06	-2.71	1	high-affinity nitrate transporter 2.1-like
TraesCS6A02G033200	-6.79	8.35E-06	-3.36	1	High affinity nitrate transporter 2.4
TraesCS6A02G267700	0.30	0.62	-1.13	4.90E-05	protein NRT1/ PTR FAMILY 8.3-like
TraesCS6A02G369900	4.75	0.01	0.22	0.93	protein NRT1/ PTR FAMILY 8.3-like isoform X1
TraesCS6B02G044100	0.06	0.90	1.51	4.09E-05	high affinity nitrate transporter
TraesCS6B02G044200	-1.21	2.49E-05	0.42	0.39	high-affinity nitrate transporter 2.1-like
TraesCS6B02G044400	-1.37	6.30E-07	0.93	0.01	high-affinity nitrate transporter 2.1-like
TraesCS6B02G044500	0.17	0.72	3.46	2.47E-36	high affinity nitrate transporter
TraesCS6B02G309200	-1.09	0.10	-2.04	0.008	protein NRT1/ PTR FAMILY 7.3-like
TraesCS6D02G035900	-2.25	6.07E-16	-0.22	0.69	high-affinity nitrate transporter 2.1-like
TraesCS6D02G037800	-3.88	0.02	-3.59	0.23	high-affinity nitrate transporter 2.1-like
TraesCS6D02G132100	1.45	0.008	1.18	0.09	protein NRT1/ PTR FAMILY 8.3-like

NN and LN indicate normal- and low-nitrogen conditions, respectively. AA and BB indicate the A-NIL and the B-NIL, respectively. The expression levels between the A-NIL and the B-NIL were compared under each condition, with the latter as a control. The expression ratios are presented as log_2FC values. Genes with a $log_2FC \leq -1$ (*p*-adjusted < 0.05, coloured blue) represent the genes whose expression was downregulated under LN conditions, and genes with $log_2FC \geq 1$ (*p*-adjusted < 0.05, coloured red) represent the genes whose expression was upregulated under LN conditions.

Gene_id	log_2FC (LN_AA/NN_AA)	*p*-adjusted	log_2FC (LN_BB/NN_BB)	*p*-adjusted	NR_description
TraesCS7A02G121600	1.87	4.14E-10	0.60	0.24	protein NRT1/ PTR FAMILY 2.3-like
TraesCS7A02G301700	-1.26	5.33E-12	-0.96	3.48E-08	protein NRT1/ PTR FAMILY 6.3-like
TraesCS7B02G262200	0.99	2.59E-05	1.16	2.16E-08	protein NRT1/ PTR FAMILY 4.6-like
TraesCS7B02G283400	0.93	0.0001	1.31	0.0001	protein NRT1/ PTR FAMILY 8.3-like
TraesCS7D02G049300	0.71	0.16	1.80	0.004	protein NRT1/ PTR FAMILY 2.3-like
TraesCS7D02G357300	1.11	2.26E-06	0.83	0.0003	protein NRT1/ PTR FAMILY 4.6-like

NN and LN indicate normal- and low-nitrogen conditions, respectively. AA and BB indicate the A-NIL and the B-NIL, respectively. The expression levels between the A-NIL and the B-NIL were compared under each condition, with the latter as a control. The expression ratios are presented as log_2FC values. Genes with a $log_2FC \leq -1$ (*p*-adjusted < 0.05, coloured blue) represent the genes whose expression was downregulated under LN conditions, and genes with $log_2FC \geq 1$ (*p*-adjusted < 0.05, coloured red) represent the genes whose expression was upregulated under LN conditions.

Phytohormones, together with their receptors and signalling components, constitute the main intrinsic regulatory pathways of root traits. Ethylene, whose biosynthesis is regulated by several key enzymes, such as 1-aminocyclopropane-1-carboxylic acid (ACC) synthase (ACS) and ACC oxidase (ACO), usually plays a negative regulatory role in root growth, inhibiting root enlargement and root meristem cell proliferation [46–49]. In addition, ethylene regulates the expression of glutathione S-transferase (GST)-encoding genes. GST catalyses the conjugation of glutathione to various electrophilic compounds involved in the oxidative stress response, crosstalk with other hormones and drought-induced root growth [50–51]. Under both NN and LN conditions, significant increases in expression levels of genes encoding ACOs and GSTs were detected in the B-NIL, with parallel increases in expression levels of genes encoding ethylene-responsive TFs (Table 4), implying that enhanced ethylene signalling together with glutathione metabolism negatively regulates root growth in the B-NIL. GA, whose catabolism is catalysed by GA2-oxidase, is considered a negative regulator of lateral root formation [52–53]. However, overexpression of GA2-oxidase-encoding genes led to shortened primary root length, and mutations in these kinds of genes led to somewhat longer roots [54–55], indicating a negative correlation between GA2-oxidase-encoding genes and root length. Compared to the A-NIL, the B-NIL displayed upregulated expression levels of several GA2-oxidase-encoding genes under both NN and LN conditions (Table 4); these upregulated levels may have inhibitory effects on root development. Brassinosteroids (BRs) regulate both root meristem size and cell expansion in controlling root growth. Deficiency or insensitivity of BRs leads to reduced root growth and lateral root formation [56]. The decreased expression of receptor-like protein kinase BRI1-like 3 genes in the B-NIL may impair BR signalling and inhibit root enlargement (Table 4). Auxin facilitates lateral root initiation and development [57–58], while cytokinin antagonistically negatively regulates root growth [59]. Members of the *GH3* gene family respond to auxin and their encoding products use various amino acids as substrates to form indole-acetic acid (IAA)-amido conjugates for temporary storage and degradation [60]. Cytokinin is activated by phosphoribohydrolase, which catalyses the hydrolysis of the bond between N^6-substituted bases and ribose 5'-monophosphates in cytokinin

precursors during its biosynthesis process [61–62] and is irreversibly degraded by cytokinin oxidase dehydrogenase [63]. Significant increases in expression levels were observed for genes encoding GH3.8 and phosphoribohydrolase in the B-NIL, accompanied by decreased expression levels of a gene encoding an auxin-responsive protein (Table 4), implying the presence of weakened auxin signalling and accelerated cytokinin flux in the B-NIL, which may be related to the differences in root traits.

Table 4
DEGs involved in phytohormone metabolism and signalling between the pairwise NILs

Gene_id	log_2FC (NN_AA/NN_BB)	*p*-adjusted	log_2FC (LN_AA/LN_BB)	*p*-adjusted	NR_description
Ethylene					
TraesCS1A02G370400	-5.05	0.0004	-2.53	5.63E-05	ethylene-responsive transcription factor ERF109-like
TraesCS1A02G370600	-3.55	4.19E-17	-1.44	8.02E-05	AP2 domain containing protein
TraesCS1A02G370700	-5.28	1.08E-51	-2.08	8.05E-11	ethylene-responsive transcription factor ERF109-like
TraesCS1B02G117400	-1.32	5.13E-05	-1.44	6.19E-09	1-aminocyclopropane-1-carboxylate oxidase-like
TraesCS1B02G389700	-3.15	3.17E-20	-1.49	6.98E-06	ethylene responsive transcription factor 6
TraesCS1B02G389800	-3.64	1.61E-26	-1.78	1.94E-07	ethylene-responsive transcription factor ERF109-like
TraesCS1D02G098000	-1.80	2.67E-11	-1.77	5.13E-10	1-aminocyclopropane-1-carboxylate oxidase-like
TraesCS1D02G098100	-1.10	8.10E-06	-1.51	7.25E-09	1-aminocyclopropane-1-carboxylate oxidase-like
TraesCS1D02G376500	-4.11	8.13E-33	-1.79	7.68E-08	ethylene-responsive transcription factor ERF109-like
TraesCS1D02G376600	-3.26	2.22E-37	-1.33	0.0001	ethylene-responsive transcription factor ERF109-like
TraesCS1D02G376700	-3.34	1.30E-23	-1.36	2.22E-05	ethylene-responsive transcription factor ERF109-like
TraesCS1D02G376800	-4.79	1.53E-42	-2.08	0.0005	ethylene-responsive transcription factor ERF109-like
TraesCS2D02G397100	-5.47	0.0002	-2.92	4.59E-09	ethylene-responsive transcription factor ERF025-like

NN and LN indicate normal- and low-nitrogen conditions, respectively. AA and BB indicate the A-NIL and the B-NIL, respectively. The expression levels between the A-NIL and the B-NIL were compared under each condition, with the latter as a control. The expression ratios are presented as log_2FC values. Genes with a $log_2FC \leq -1$ (*p*-adjusted < 0.05, coloured blue) represent the genes whose expression was downregulated in the A-NIL, and genes with $log_2FC \geq 1$ (*p*-adjusted < 0.05, coloured red) represent the genes whose expression was upregulated in the A-NIL.

Gene_id	log_2FC (NN_AA/NN_BB)	*p*-adjusted	log_2FC (LN_AA/LN_BB)	*p*-adjusted	NR_description
TraesCS3B02G158800	1.56	0.037	1.89	0.003	AP2 domain transcription factor TaDREB2
TraesCS3B02G412500	-2.39	4.76E-05	-1.17	0.046	F-box domain containing protein, expressed
TraesCS4A02G256500	-4.94	5.60E-08	-4.57	5.50E-19	1-aminocyclopropane-1-carboxylate synthase 1-like
TraesCS4B02G058200	-2.51	7.59E-09	-3.30	5.16E-23	1-aminocyclopropane-1-carboxylate synthase 1-like
TraesCS4D02G058200	-2.67	1.16E-12	-2.89	1.08E-23	1-aminocyclopropane-1-carboxylate synthase 1-like
TraesCS4D02G096400	-1.62	8.07E-10	-1.25	2.91E-11	lipase-like PAD4
TraesCS5B02G236900	-2.68	6.45E-17	-1.25	0.0009	ethylene-responsive transcription factor ERF109-like
TraesCS5D02G245300	-2.37	2.30E-10	-1.34	0.002	ethylene-responsive transcription factor ERF109-like
TraesCS6A02G235100	1.95	5.71E-07	1.08	0.004	predicted protein
TraesCS6A02G256600	-3.44	9.28E-14	-2.30	4.23E-12	ethylene-responsive transcription factor ERF027-like
TraesCS6A02G319500	-3.88	2.62E-11	-2.36	1.01E-09	ethylene-responsive transcription factor ERF109-like
TraesCS6A02G330500	-1.83	5.11E-16	-1.26	1.25E-06	ethylene-responsive transcription factor ERF014-like
TraesCS6B02G268700	-3.01	3.89E-17	-2.22	1.77E-19	ethylene-responsive transcription factor ERF027-like
TraesCS6B02G281000	-1.76	4.23E-09	-1.36	1.78E-07	ethylene-responsive transcription factor 1-like

NN and LN indicate normal- and low-nitrogen conditions, respectively. AA and BB indicate the A-NIL and the B-NIL, respectively. The expression levels between the A-NIL and the B-NIL were compared under each condition, with the latter as a control. The expression ratios are presented as log_2FC values. Genes with a $log_2FC \leq -1$ (*p*-adjusted < 0.05, coloured blue) represent the genes whose expression was downregulated in the A-NIL, and genes with $log_2FC \geq 1$ (*p*-adjusted < 0.05, coloured red) represent the genes whose expression was upregulated in the A-NIL.

Gene_id	log_2FC (NN_AA/NN_BB)	*p*-adjusted	log_2FC (LN_AA/LN_BB)	*p*-adjusted	NR_description
TraesCS6B02G350100	-4.04	9.00E-12	-2.71	5.23E-10	ethylene-responsive transcription factor ERF109-like
TraesCS6B02G350400	-3.41	7.85E-42	-1.71	5.20E-07	ethylene-responsive transcription factor ERF109-like
TraesCS6B02G361400	-2.21	9.84E-22	-1.05	9.84E-08	ethylene-responsive transcription factor ERF014-like
TraesCS6D02G217800	1.72	1.14E-05	1.02	0.0004	ethylene-responsive transcription factor ERF054-like
TraesCS6D02G237800	-3.23	2.79E-19	-2.32	1.03E-21	ethylene-responsive transcription factor ERF027-like
TraesCS6D02G298700	-3.68	1.54E-06	-2.41	3.40E-09	ethylene-responsive transcription factor ERF109-like
TraesCS6D02G299000	-4.6422	0.007	-2.09	0.0022	ethylene-responsive transcription factor ERF109-like
TraesCS6D02G299100	-3.71	2.77E-37	-1.96	2.11E-06	ethylene-responsive transcription factor ERF109-like
TraesCS6D02G309600	-1.66	1.08E-15	-1.13	3.56E-05	ethylene-responsive transcription factor ERF014-like
glutathione S-transferase					
TraesCS1B02G194100	-1.22	0.002	-1.11	0.0006	putative glutathione S-transferase GSTU6
TraesCS1B02G194500	-1.36	0.0005	-1.25	0.046	probable glutathione S-transferase GSTU6
TraesCS2A02G218700	-4.72	9.96E-19	-2.78	5.22E-20	probable glutathione S-transferase GSTU6
TraesCS2B02G244100	-3.87	3.27E-19	-2.39	6.06E-19	probable glutathione S-transferase GSTU6
TraesCS2B02G322800	-1.38	1.14E-06	-1.19	9.82E-05	glutathione S-transferase TCHQD

NN and LN indicate normal- and low-nitrogen conditions, respectively. AA and BB indicate the A-NIL and the B-NIL, respectively. The expression levels between the A-NIL and the B-NIL were compared under each condition, with the latter as a control. The expression ratios are presented as log_2FC values. Genes with a $log_2FC \leq -1$ (*p*-adjusted < 0.05, coloured blue) represent the genes whose expression was downregulated in the A-NIL, and genes with $log_2FC \geq 1$ (*p*-adjusted < 0.05, coloured red) represent the genes whose expression was upregulated in the A-NIL.

Gene_id	log_2FC (NN_AA/NN_BB)	*p*-adjusted	log_2FC (LN_AA/LN_BB)	*p*-adjusted	NR_description
TraesCS2D02G044100	-3.99	0.03	-2.58	0.002	probable glutathione S-transferase GSTF1
TraesCS2D02G224700	-1.83	0.001	-1.72	5.55E-08	probable glutathione S-transferase GSTU6
TraesCS2D02G304500	-1.58	9.35E-06	-1.45	8.40E-12	glutathione S-transferase TCHQD
TraesCS3A02G309100	-1.92	5.18E-06	-1.14	4.15E-05	unnamed protein product
TraesCS3D02G130700	1.39	0.006	1.16	0.0006	probable glutathione S-transferase GSTU6
TraesCS3D02G486100	-1.15	9.69E-05	-1.07	3.18E-07	glutathione transferase GST 23-like
Gibberellin					
TraesCS1A02G334400	-1.81	2.73E-09	-2.32	3.52E-16	gibberellin 2-oxidase
TraesCS2A02G189600	-1.61	3.52E-11	-1.29	5.11E-09	chitin-inducible gibberellin-responsive protein 2-like
TraesCS2B02G217500	-1.59	8.03E-14	-1.32	1.55E-09	chitin-inducible gibberellin-responsive protein 2-like
TraesCS2B02G239400	-1.24	5.27E-08	-1.03	3.57E-05	chitin-inducible gibberellin-responsive protein 1
TraesCS2D02G198200	-1.36	5.50E-11	-1.46	1.23E-10	chitin-inducible gibberellin-responsive protein 2-like
TraesCS2D02G220200	-1.33	2.10E-10	-1.03	9.21E-07	chitin-inducible gibberellin-responsive protein 1
TraesCS3A02G122600	1.25	0.04	1.67	3.54E-07	gibberellin 3-oxidase 2 – 1
TraesCS3A02G294000	-1.73	2.71E-09	-1.45	9.93E-17	gibberellin 2-oxidase
TraesCS3B02G328700	-1.86	1.62E-08	-1.71	3.62E-07	gibberellin 2-oxidase 3 isozyme B1

NN and LN indicate normal- and low-nitrogen conditions, respectively. AA and BB indicate the A-NIL and the B-NIL, respectively. The expression levels between the A-NIL and the B-NIL were compared under each condition, with the latter as a control. The expression ratios are presented as log_2FC values. Genes with a $log_2FC \leq -1$ (*p*-adjusted < 0.05, coloured blue) represent the genes whose expression was downregulated in the A-NIL, and genes with $log_2FC \geq 1$ (*p*-adjusted < 0.05, coloured red) represent the genes whose expression was upregulated in the A-NIL.

Gene_id	log_2FC (NN_AA/NN_BB)	*p*-adjusted	log_2FC (LN_AA/LN_BB)	*p*-adjusted	NR_description
TraesCS6A02G221900	-2.35	1.36E-13	-2.00	1.46E-10	gibberellin-2-oxidase-A9
TraesCS6D02G213100	-2.84	2.58E-08	-3.35	3.80E-17	gibberellin 2-beta-dioxygenase 8-like
Brassinosteroid					
TraesCS2A02G142300	1.42	4.85E-05	1.077	7.91E-05	probable cytochrome P450 313a4
TraesCS3B02G550900	-2.31	0.004	-1.70	0.0004	protein BRASSINOSTEROID INSENSITIVE 1-like isoform X1
TraesCS5B02G174400	1.24	9.18E-07	1.43	1.95E-07	receptor-like protein kinase BRI1-like 3
TraesCS5D02G181500	1.32	1.42E-07	1.56	4.46E-14	receptor-like protein kinase BRI1-like 3
Auxin					
TraesCS2A02G183900	-1.73	1.42E-12	-1.43	1.77E-13	probable indole-3-acetic acid-amido synthetase GH3.8
TraesCS5A02G378300	1.42	0.0498	1.12	3.10E-05	Auxin-responsive protein IAA30
TraesCS6B02G359400	-1.38	0.001	-1.07	0.005	predicted protein, partial
Cytokinin					
TraesCS1A02G156100	-3.19	2.83E-07	-2.22	3.79E-14	probable cytokinin riboside 5'-monophosphate phosphoribohydrolase LOGL10 isoform X1
TraesCS3D02G475800	-2.54	4.52E-07	-1.43	6.95E-05	cytokinin dehydrogenase 4-like

NN and LN indicate normal- and low-nitrogen conditions, respectively. AA and BB indicate the A-NIL and the B-NIL, respectively. The expression levels between the A-NIL and the B-NIL were compared under each condition, with the latter as a control. The expression ratios are presented as log_2FC values. Genes with a $log_2FC \leq -1$ (*p*-adjusted < 0.05, coloured blue) represent the genes whose expression was downregulated in the A-NIL, and genes with $log_2FC \geq 1$ (*p*-adjusted < 0.05, coloured red) represent the genes whose expression was upregulated in the A-NIL.

Several types of TFs play essential roles in root growth by regulating the expression of downstream genes that are usually closely associated with nutrient acquisition. Conserved nuclear transcription factor Y (NF-Y) comprises 3 subunits, NF-YA, NF-YB and NF-YC, and regulates photosynthesis [64–65], nodule development [66], plant flowering [67–68], seed development [69] and tolerance to abiotic stresses [70–72] in eukaryotes. Overexpression of *TaNFYA-B1* was shown to increase both primary root length and total lateral root length in wheat [22]. The expression levels

of genes encoding NF-Y subunit C-3-like proteins (TraesCS1A02G354900, TraesCS1B02G366800 and TraesCS1D02G355600) were higher in the A-NIL than in the B-NIL under LN condition (Table 5), indicating their potential contribution to LN-induced root enlargement. Plant-specific NAM, ATAF and CUC (NAC) TFs are characterized by a highly conserved DNA-binding domain and variable C-terminal domains [73]. NAC TFs function not only in response to stresses [74] but also in response to NO_3-, depending on the NRT1.1 NO_3^- transport function [75], and to increase root biomass [21]. Two genes encoding NAC TFs (TraesCS3A02G078400 and TraesCS3D02G078900) exhibited higher expression levels in the A-NIL than in the B-NIL under both NN and LN conditions (Table 5), implying that they have similar effects on root growth.

Table 5
Differentially expressed TF-encoding genes between the pairwise NILs

Gene_id	log_2FC (NN_AA/NN_BB)	*p*-adjusted	log_2FC (LN_AA/LN_BB)	*p*-adjusted	NR_description
NTF					
TraesCS1A02G354900	0.70	1	2.16	0.02	nuclear transcription factor Y subunit C-3-like
TraesCS1B02G366800	0.64	0.89	1.83	0.0007	nuclear transcription factor Y subunit C-3-like
TraesCS1D02G355600	0.45	0.95	2.60	0.003	nuclear transcription factor Y subunit C-3-like
NAC					
TraesCS3A02G078400	1.48	0.004	1.37	3.04E-07	NAC transcription factor
TraesCS3A02G339600	-3.07	3.15E-22	-3.01	1.27E-27	NAC transcription factor 4
TraesCS3D02G078900	1.79	6.26E-06	1.39	5.36E-05	NAC transcription factor

NN and LN indicate normal- and low-nitrogen conditions, respectively. AA and BB indicate the A-NIL and the B-NIL, respectively. The expression levels between the A-NIL and the B-NIL were compared under each condition, with the latter as a control. The expression ratios are presented as log_2FC values. Genes with a $log_2FC \leq -1$ (*p*-adjusted < 0.05, coloured blue) represent the genes whose expression was downregulated in the A-NIL, and genes with $log_2FC \geq 1$ (*p*-adjusted < 0.05, coloured red) represent the genes whose expression was upregulated in the A-NIL.

In conclusion, transcriptomic analysis in the present study revealed the landscape of the genes differentially expressed between the NILs with different *QMrl-7B* alleles under both NN and LN conditions, reflecting the physiological basis of the large roots of the superior parent KN9204. This study used pairwise NILs for analysis to dampen the effects from different genetic backgrounds; as such, the DEGs are more likely to be related to *QMrl-7B*, either directly or indirectly. These results revealed many pathways regulated by genes that interact genetically with *QMrl-7B*, which may provide a foundation for the application of *QMrl-7B* in molecular breeding. However, since the materials used for RNA-seq were seedlings and not mature plants, much work is still needed to elucidate the overall genetic network that controls ideal root traits of plants at different stages.

Methods

Plant materials and root phenotyping

KN9204 is a representative cultivar released in 2003 with a prolific root system, and J411 is a major cultivar that has been planted on the Northern China Plain since the 1990s [30]. A major stable QTL, *QMrl-7B* (which controls MRL), and two types of *QMrl-7B* NILs, one with superior alleles from KN9204 (referred to as the A-NIL) and another with inferior alleles from J411 (referred to as the B-NIL) were described by Fan et al. [15]. Compared with the B-NIL, the A-NIL produces a larger root system and have a higher nitrogen use efficiency (NUE) in hydroponic culture [15] and in field trials under different N levels (Liu et al., in revision). These pairwise NILs were used in this study for transcriptomic analysis.

To evaluate the root morphological traits, experiments involving different N hydroponic cultures were carried out to characterize the pairwise *QMrl-7B* NILs, with three replications. Seeds were imbibed in distilled water at 23°C for 24 h and then transferred to plastic pots containing moist vermiculite and nutrient-enriched soil (1:1, v/v) for ten days. Uniform seedlings (at the one- and half-leaf stages) were then chosen, after which their residual endosperm was removed; they were subsequently cultured in both normal-nitrogen (NN) and low-nitrogen (LN) nutrient solutions as described by Fan et al. [15]. On the fourteenth (four-leaf stage) and twenty-first (five-leaf stage) days in different N hydroponic cultures, five uniform seedlings of each NIL were evaluated for their average MRL, total root length (TRL, cm), RA (cm^2) and RV (cm^3). MRL was measured using a ruler, and the remaining traits (TRL, RA and RV) were quantified by using a ScanMaker i800 Plus Scanner (600 DPI) and analysed by LA-S software (Hangzhou Wanshen Detection Technology Co., Ltd., Hangzhou, China; www.wseen.com).

Moreover, the roots of the four-leaf-stage seedlings of the pairwise NILs were sampled and immediately frozen in liquid N for subsequent RNA extraction. The root samples were divided into four treatments: the A-NIL under NN condition (NN_AA), the B-NIL under NN condition (NN_BB), the A-NIL under LN condition (LN_AA) and the B-NIL under LN condition (LN_BB). Each sample pool comprised five individual seedlings, and all experiments were replicated three times.

Transcriptome analysis

RNA extraction and sequencing

Total RNA was extracted from the root samples using TRIzol Reagent (Plant RNA Purification Reagent for plant tissue, Invitrogen, USA) according to the manufacturer's instructions, and genomic DNA was removed using DNase I (TaKaRa). The quantity, quality, and integrity of the extracted RNA were determined using an ND-2000 spectrophotometer (NanoDrop Technology, USA) and an Agilent 2100 Bioanalyzer (Agilent Technologies, Santa Clara, CA, USA). Only high-quality RNA samples (OD260/280 = 1.8~2.2, OD260/230 ≥ 2.0, RNA integrity number (RIN) ≥ 6.5, 28S:18S ≥ 1.0, > 1 μg) were used to construct a sequencing library. Messenger RNA (mRNA) was isolated from the total RNA using magnetic beads with oligo (dT) primers and then cut into short fragments in fragmentation buffer. Complementary DNA (cDNA) was subsequently synthesized using a SuperScript Double-Stranded cDNA Synthesis Kit (Invitrogen, CA, USA), with random hexamer primers (Illumina). The synthesized cDNA was then subjected to end repair, phosphorylation and polyadenylation according to Illumina's library construction protocol. The libraries were size selected for cDNA target fragments of 300 bp on 2% low-range ultra-agarose followed by PCR amplification using Phusion DNA polymerase (NEB); 15 PCR cycles were performed. After quantification by a TBS-380 fluorometer, the paired-end RNA-seq library was sequenced with an Illumina HiSeq

Xten/NovaSeq 6000 sequencer (2 × 150 bp read length). The library was then sequenced using the Illumina HiSeq^{TM} platform (Shanghai Majorbio Bio-pharm Technology Co., Ltd., Shanghai, China).

Analysis of DEGs

The data were analysed on the free online platform of the Majorbio Cloud Platform (www.majorbio.com). To obtain high-quality reads, reads containing adapter sequences and reads of low quality were removed from the raw data to obtain clean reads in FASTQ format. Q20 and Q30 values and GC contents were determined according to conventional methods. Afterwards, the remaining clean reads were mapped to the reference genome of Chinese Spring (CS) (http://plants.ensembl.org/Triticum_aestivum/Info/Index/) by HISAT2 software (http://ccb.jhu.edu/software/hisat2/index.shtml). Unigene expression levels were estimated according to their transcripts per million reads mapped (TPM) values. DEGs between the A-NIL and the B-NIL under both NN and LN conditions were then analysed using the DESeq2 package [76], and the expression results are presented in terms of the $\log_2$fold change (FC). $|\log_2 FC| \geq 1$ and *p*-adjusted < 0.05 were used as thresholds to judge the significance of gene expression differences. DEGs were also evaluated in response to LN stress for each NIL.

The DEGs of each one-to-one comparison were analysed by Gene Ontology (GO) and Kyoto Encyclopedia of Genes and Genomes (KEGG) pathway enrichment analysis. GO functional enrichment and KEGG pathway analysis were carried out by Goatools (https://github.com/tanghaibao/Goatools) and KOBAS (http://kobas.cbi.pku.edu.cn/home.do), where GO terms and biological pathways with a *p*-adjusted < 0.05 were considered significantly enriched. The encoded products of the DEGs were subsequently annotated by the NCBI non-redundant protein (NR) database.

Quantitative real-time polymerase chain reaction (qRT-PCR) validation

To confirm the reliability of the DEGs obtained from RNA-seq, eight DEGs on chromosome 7B were selected for qRT-PCR analysis. Gene-specific primers were designed using Primer Premier 5.0 software (Premier Biosoft International); the sequences are shown in Table S1. qRT-PCR was carried out in total volumes of 20 μl using a SYBR PCR kit (TaKaRa) on an ABI 7500 real-time PCR system (Applied Biosystems, USA) according to the manufacturers' instructions. Each sample was analysed as three technical replicates, and the relative expression value of the DEGs was determined using the comparative cycle threshold (Ct) method after normalization to the expression of the GAPDH control.

Abbreviations

NN
normal-nitrogen; LN:low-nitrogen; NIL:near isogenic line; DEG:differentially expressed gene; QTL:quantitative trait locus; RNA-seq:RNA sequencing; NUE:nitrogen use efficiency; MRL:maximu m root length; TRL:total root length; RA:root surface area; RV:root volume; GO; Gene Ontology; KEGG:Kyoto Encyclopedia of Genes and Genomes;

Declarations

Acknowledgments

Not applicable.

Authors' Contributions

Liqiang Song and Xiaoli Fan planned the research project. Jiajia Liu, Hanwen Li, Xiaoli Fan, Liqiang Song, Na Zhang, Deyuan Meng, Liya Zhi, Xiaoli Ren, Jun Ji and Junming Li conducted the hydroponic culture and field experiments. Jiajia Liu, Hanwen Li, Liqiang Song, Xiaoli Fan and Zhenqi Su analyzed the data. Hanwen Li, Jiajia Liu, Liqiang Song and Xiaoli Fan wrote the manuscript, Zhenqi Su and Junming Li revised the manuscript.

Funding

This research was jointly supported by grants from the National Key Research and Development Program of China (2016YFD0100706), the Youth Innovation Promotion Association of CAS (2020364), and China Agriculture Research System (CARS-03).

Availability of data and materials

All data generated or analysed during this study are included in this published article and its supplementary information files.

Ethics approval and consent to participate

Not applicable.

Consent for publication

Not applicable.

Competing interests

The authors declare that they have no competing interests.

References

1. Khush GS. Green revolution: the way forward. Nat Rev Genet. 2001; 2: 815–822.
2. Godfray HC, Beddington JR, Crute IR, Haddad L, Lawrence D, Muir JF, Pretty J, Robinson S, Thomas SM, Toulmin C. Food security: the challenge of feeding 9 billion people. Science. 2010; 327: 812–818.
3. Raun WR, Johnson GV. Improving nitrogen use efficiency for cereal production. Agron J. 1999; 91: 357–363.
4. Springmann M, Clark M, Mason-D'Croz D, Wiebe K, Bodirsky BL, Lassaletta L, de Vries W, Vermeulen SJ, Herrero M, Carlson KM, et al. Options for keeping the food system within environmental limits. Nature. 2018; 562: 519–525.
5. Waines JG, Ehdaie B. Domestication and crop physiology: roots of green-revolution wheat. Ann Bot. 2007; 100: 991–998.
6. Meister R, Rajani MS, Ruzicka D, Schachtman DP. Challenges of modifying root traits in crops for agriculture. Trends Plant Sci. 2014; 19: 779–788.
7. Lynch JP. Roots of the second green revolution. Aust J Bot. 2007; 55: 493–512.
8. Gewin V. Food: an underground revolution. Nature. 2010; 466, 552–553.
9. Kucke M, Schmid H, Spiess A. A comparison of four methods for measuring roots of field crops in three contrasting soils. Plant Soil. 1995; 172, 63–71.

10. An DG, Su JY, Liu QY, Zhu YG, Tong YP, Li JM, Jing RL, Li B, Li ZS. Mapping QTLs for nitrogen uptake in relation to the early growth of wheat (*Triticum aestivum* L.). Plant Soil. 2006; 284: 73–84.
11. Cao P, Ren Y, Zhang K, Teng W, Zhao X, Dong Z, Liu X, Qin H, Li Z, Wang D, et al. Further genetic analysis of a major quantitative trait locus controlling root length and related traits in common wheat. Mol Breed. 2014; 33: 975–985.
12. Kabir MR, Liu G, Guan P, Wang F, Khan AA, Ni Z, Yao Y, Hu Z, Xin M, Peng H, et al. Mapping QTLs associated with root traits using two different populations in wheat (*Triticum aestivum* L.). Euphytica. 2015; 206: 175–190.
13. Maccaferri M, El-Feki W, Nazemi G, Salvi S, Canè MA, Colalongo MC, Stefanelli S, Tuberosa R. Prioritizing quantitative trait loci for root system architecture in tetraploid wheat. J Exp Bot. 2016; 67: 1161–1178.
14. Merchuk-Ovnat L, Fahima T, Ephrath JE, Krugman T, Saranga Y. Ancestral QTL alleles from wild emmer wheat enhance root development under drought in modern wheat. Front Plant Sci. 2017, 8: 703.
15. Fan X, Zhang W, Zhang N, Chen M, Zheng S, Zhao C, Han J, Liu J, Zhang X, Song L, et al. Identification of QTL regions for seedling root traits and their effect on nitrogen use efficiency in wheat (*Triticum aestivum* L.). Theore Appl Genet. 2018; 131: 2677–2698.
16. Zheng X, Wen X, Qiao L, Zhao J, Zhang X, Li X, Zhang S, Yang Z, Chang Z, Chen J, et al. A novel QTL *QTrl.saw-2D.2* associated with the total root length identified by linkage and association analyses in wheat (*Triticum aestivum* L.). Planta. 2019; 250: 129–143.
17. Han H, Wang H, Han Y, Hu Z, Xin M, Peng H, Yao Y, Sun Q, Ni Z. Altered expression of the *TaRSL2* gene contributed to variation in root hair length during allopolyploid wheat evolution. Planta. 2017; 246: 1019–1028.
18. Wang H, Hu Z, Huang K, Han Y, Zhao A, Han H, Song L, Fan C, Li R, Xin M, et al. Three genomes differentially contribute to the seedling lateral root number in allohexaploid wheat: evidence from phenotype evolution and gene expression. Plant J. 2018; 95: 976–987.
19. Hao L, Wen Y, Zhao Y, Lu W, Xiao K. Wheat mitogen-activated protein kinase gene *TaMPK4* improves plant tolerance to multiple stresses through modifying root growth, ROS metabolism, and nutrient acquisitions. Plant Cell Rep. 2015; 34: 2081–2097.
20. Li B, Liu D, Li Q, Mao X, Li A, Wang J, Chang X, Jing R. Overexpression of wheat gene *TaMOR* improves root system architecture and grain yield in Oryza sativa. J Exp Bot. 2016; 67: 4155–4167.
21. He X, Qu B, Li W, Zhao X, Teng W, Ma W, Ren Y, Li B, Li Z, Tong Y. The nitrate-inducible NAC transcription factor TaNAC2-5A controls nitrate response and increases wheat yield. Plant Physiol. 2105; 169: 1991–2005.
22. Qu B, He X, Wang J, Zhao Y, Teng W, Shao A, Zhao X, Ma W, Li B, Li Z, et al. A wheat CCAAT box-binding transcription factor increases the grain yield of wheat with less fertilizer input. Plant Physiol. 2105; 167: 411–423.
23. Chen D, Richardson T, Chai S, Lynne MC, Rae AL, Xue GP. Drought-up-regulated TaNAC69-1 is a transcriptional repressor of *TaSHY2* and *TaIAA7*, and enhances root length and biomass in wheat. Plant Cell Physiol. 2016; 57: 2076–2090.
24. Hu Z, Wang R, Zheng M, Liu X, Meng F, Wu H, Yao Y, Xin M, Peng H, Ni Z, et al. TaWRKY51 promotes lateral root formation through negative regulation of ethylene biosynthesis in wheat (*Triticum aestivum* L.). Plant J. 2018; 96: 372–388.
25. Yang J, Wang M, Li W, He X, Teng W, Ma W, Zhao X, Hu M, Li H, Zhang Y, et al. Reducing expression of a nitrate-responsive bZIP transcription factor increases grain yield and N use in wheat. Plant Biotechnol J. 2019; 17: 1823–1833.

26. Xu Y, Ren Y, Lin T, Cui D. Identification and characterization of CircRNAs involved in the regulation of wheat root length. Biol Res. 2019; 52: 19.
27. Hu L, Li H, Chen L, Lou Y, Amombo E, Fu J. RNA-seq for gene identification and transcript profiling in relation to root growth of bermudagrass (Cynodon dactylon) under salinity stress. BMC Genomics. 2015; 16: 575.
28. He X, Ma H, Zhao X, Nie S, Li Y, Zhang Z, Shen Y, Chen Q, Lu Y, Lan H, et al. Comparative RNA-seq analysis reveals that regulatory network of maize root development controls the expression of genes in response to N stress. PLoS One. 2016; 11: e0151697.
29. Han Y, Gao Y, Shi Y, Du J, Zheng D, Liu G. Genome-wide transcriptome profiling reveals the mechanism of the effects of uniconazole on root development in Glycine max. J Plant Biol. 2017; 60: 387–403.
30. Wang RF, An DG, Hu CS, Li LH, Zhang YM, Jia YG, Tong YP. Relationship between nitrogen uptake and use efficiency of winter wheat grown in the North China Plain. Crop Pasture Sci. 2011; 62: 504–514.
31. Schopfer P. Hydroxyl radical-induced cell-wall loosening in vitro and in vivo: implications for the control of elongation growth. Plant J. 2001; 28: 679–688.
32. Liszkay A, Zalm EVD, Schopfer P. Production of reactive oxygen intermediates ($O_2.^-$, H_2O_2, and .OH) by maize roots and their role in wall loosening and elongation growth. Plant Physiol. 2004; 136: 3114–3123.
33. Cosio C, Dunand C. Specific functions of individual class III peroxidase genes. J Exp Bot. 2009; 60: 391–408.
34. Li J, Su L, Lv A, Li Y, Zhou P, An Y. MsPG1 alleviated aluminum-induced inhibition of root growth by decreasing aluminum accumulation and increasing porosity and extensibility of cell walls in alfalfa (*Medicago sativa*). Environ Exp Bot. 2020; 175.
35. Vogt T. Phenylpropanoid biosynthesis. Mol Plant. 2010; 3: 2–20.
36. Liu H, Wang Z, Xu W, Zeng J, Li L, Li S, Gao Z. Bacillus pumilus LZP02 promotes rice root growth by improving carbohydrate metabolism and phenylpropanoid biosynthesis. Mol Plant Microbe Interact. 2020; 33: 1222–1231.
37. Muro-Villanueva F, Mao X, Chapple C. Linking phenylpropanoid metabolism, lignin deposition, and plant growth inhibition. Curr Opin Biotechnol. 2019; 56: 202–208.
38. Crawford NM, Glass ADM. Molecular and physiological aspects of nitrate uptake in plants. Trends Plant Sci. 1998; 3: 389–395.
39. Zhang H, Forde BG. An Arabidopsis MADS box gene that controls nutrient-induced changes in root architecture. Science. 1998; 279: 407–409.
40. Remans T, Nacry P, Pervent M, Filleur S, Diatloff E, Mounier E, Tillard P, Forde BG, Gojon A. The *Arabidopsis* NRT1.1 transporter participates in the signaling pathway triggering root colonization of nitrate-rich patches. Proc Natl Acad Sci. 2006; 103: 19206–19211.
41. Ho CH, Lin SH, Hu HC, Tsay YF. CHL1 functions as a nitrate sensor in plants. Cell. 2009; 138: 1184–1194.
42. Krouk G, Lacombe B, Bielach A, Perrine-Walker F, Malinska K, Mounier E, Hoyerova K, Tillard P, Leon S, Ljung K, et al. Nitrate-regulated auxin transport by NRT1.1 defines a mechanism for nutrient sensing in plants. Dev Cell. 2010; 18: 927–937.
43. Wang YY, Hsu PK, Tsay YF. Uptake, allocation and signaling of nitrate. Trends Plant Sci. 2012; 17: 458–467.
44. Tal I, Zhang Y, Jorgensen ME, Pisanty O, Barbosa ICR, Zourelidou M, Regnault T, Crocoll C, Olsen CE, Weinstain R, et al. The *Arabidopsis* NPF3 protein is a GA transporter. Nat Commun. 2016; 7.
45. Gelli M, Duo Y, Konda AR, Zhang C, Holding D, Dweikat I. Identification of differentially expressed genes between sorghum genotypes with contrasting nitrogen stress tolerance by genome-wide transcriptional

profiling. BMC Genomics. 2014; 15.

46. Cary AJ, Liu W, Howell SH. Cytokinin action is coupled to ethylene in its effects on the inhibition of root and hypocotyl elongation in *Arabidopsis thaliana* seedlings. Plant Physiol. 1995; 107: 1075–1082.
47. Chae HS, Faure F, Kieber JJ. The *eto1*, *eto2*, and *eto3* mutations and cytokinin treatment increase ethylene biosynthesis in *Arabidopsis* by increasing the stability of ACS protein. Plant Cell. 2003; 15: 545–559.
48. Street IH, Aman S, Zubo Y, Ramzan A, Wang X, Shakeel SN, Kieber JJ, Schaller GE. Ethylene inhibits cell proliferation of the *Arabidopsis* root meristem. Plant Physiol. 2015; 169: 338–350.
49. Pattyn J, Vaughan-Hirsch J, and Poel BVD. The regulation of ethylene biosynthesis: a complex multilevel control circuitry. New Phytol. 2020;
50. Mang HG, Kang EO, Shim JH, Kim SY, Park KY, Kim YS, Bahk YY, Kim WT. A proteomic analysis identifies glutathione S-transferase isoforms whose abundance is differentially regulated by ethylene during the formation of early root epidermis in *Arabidopsis* seedlings. Biochim Biophys Acta. 2004; 1676: 231–239.
51. Dalal M, Sahu S, Tiwari S, Rao AR, Gaikwad K. Transcriptome analysis reveals interplay between hormones, ROS metabolism and cell wall biosynthesis for drought-induced root growth in wheat. Plant Physiol Biochem. 2018; 130: 482–492.
52. Olszewski N, Sun TP, Gubler F. Gibberellin signaling: biosynthesis, catabolism, and response pathways. Plant Cell. 2002; 14 Suppl: S61-80.
53. Gou J, Strauss SH, Tsai CJ, Fang K, Chen Y, Jiang X, Busov VB. Gibberellins regulate lateral root formation in Populus through interactions with auxin and other hormones. Plant Cell. 2010; 22: 623–639.
54. Li H, Torres-Garcia J, Latrasse D, Benhamed M, Schilderink S, Zhou W, Kulikova O, Hirt H, Bisseling T. Plant-specific histone deacetylases HDT1/2 regulate GIBBERELLIN 2-OXIDASE2 expression to control Arabidopsis root meristem cell number. Plant Cell. 2017; 29: 2183–2196.
55. Rieu I, Eriksson S, Powers SJ, Gong F, Griffiths J, Woolley L, Benlloch R, Nilsson O, Thomas SG, Hedden P, et al. Genetic analysis reveals that C19-GA 2-oxidation is a major gibberellin inactivation pathway in Arabidopsis. Plant Cell. 2008; 20: 2420–2436.
56. Wei Z, Li J. Brassinosteroids regulate root growth, development, and symbiosis. Mol Plant. 2016; 9: 86–100.
57. Forde BG. Local and long-range signaling pathways regulating plant responses to nitrate. Annu Rev Plant Biol. 2002; 53: 203–224.
58. Fukaki H, Tasaka M. Hormone interactions during lateral root formation. Plant Mol Biol. 2009; 69: 437–449.
59. Moubayidin L, Di Mambro R, Sabatini S. Cytokinin-auxin crosstalk. Trends Plant Sci. 2009; 14: 557–562.
60. Staswick PE, Serban B, Rowe M, Tiryaki I, Maldonado MT, Maldonado MC, Suza W. Characterization of an *Arabidopsis* enzyme family that conjugates amino acids to indole-3-acetic acid. Plant Cell. 2005; 17: 616–627.
61. Kurakawa T, Ueda N, Maekawa M, Kobayashi K, Kojima M, Nagato Y, Sakakibara H, Kyozuka J. Direct control of shoot meristem activity by a cytokinin-activating enzyme. Nature. 2007; 445: 652–655.
62. Kuroha T, Tokunaga H, Kojima M, Ueda N, Ishida T, Nagawa S, Fukuda H, Sugimoto K, Sakakibara H. Functional analyses of LONELY GUY cytokinin-activating enzymes reveal the importance of the direct activation pathway in *Arabidopsis*. Plant Cell. 2009; 21: 3152–3169.
63. Galuszka P, Frebort I, Sebela M, Sauer P, Jacobsen S, Pec P. Cytokinin oxidase or dehydrogenase? Mechanism of cytokinin degradation in cereals. Eur J Biochem. 2001; 268: 450–461.
64. Stephenson TJ, McIntyre CL, Collet C, Xue GP. TaNF-YB3 is involved in the regulation of photosynthesis genes in *Triticum aestivum*. Funct Integr Genomics. 2011; 11: 327–340.

65. Stephenson TJ, McIntyre CL, Collet C, Xue GP. TaNF-YC11, one of the light-upregulated NF-YC members in *Triticum aestivum*, is co-regulated with photosynthesis-related genes. Funct Integr Genomics. 2010; 10: 265–276.
66. Zanetti ME, Blanco FA, Beker MP, Battaglia M, Aguilar OM. A C subunit of the plant nuclear factor NF-Y required for rhizobial infection and nodule development affects partner selection in the common bean-Rhizobium etli symbiosis. Plant Cell. 2010; 22: 4142–4157.
67. Wei X, Xu J, Guo H, Jiang L, Chen S, Yu C, Zhou Z, Hu P, Zhai H, Wan J. DTH8 suppresses flowering in rice, influencing plant height and yield potential simultaneously. Plant Physiol. 2010; 153: 1747–1758.
68. Li C, Distelfeld A, Comis A, Dubcovsky J. Wheat flowering repressor VRN2 and promoter CO2 compete for interactions with NUCLEAR FACTOR-Y complexes. Plant J. 2011; 67: 763–773.
69. Yamamoto A, Kagaya Y, Toyoshima R, Kagaya M, Takeda S, Hattori T. Arabidopsis NF-YB subunits LEC1 and LEC1-LIKE activate transcription by interacting with seed-specific ABRE-binding factors. Plant J. 2009; 58: 843–856.
70. Nelson DE, Repetti PP, Adams TR, Creelman RA, Wu J, Warner DC, Anstrom DC, Bensen RJ, Castiglioni PP, Donnarummo MG, et al. Plant nuclear factor Y (NF-Y) B subunits confer drought tolerance and lead to improved corn yields on water-limited acres. Proc Natl Acad Sci. 2007; 104: 16450–16455.
71. Zhao B, Ge L, Liang R, Li W, Ruan K, Lin H, Jin Y. Members of miR-169 family are induced by high salinity and transiently inhibit the NF-YA transcription factor. BMC Mol Biol. 2009; 10: 29.
72. Shi H, Ye T, Zhong B, Liu X, Jin R, Chan Z. AtHAP5A modulates freezing stress resistance in *Arabidopsis* through binding to CCAAT motif of AtXTH21. New Phytol. 2014; 203: 554–567.
73. Ooka H, Satoh K, Doi K, Nagata T, Otomo Y, Murakami K, Matsubara K, Osato N, Kawai J, Carninci P, et al. Comprehensive analysis of NAC family genes in Oryza sativa and *Arabidopsis thaliana*. DNA Res. 2003; 10: 239–247.
74. Nakashima K, Takasaki H, Mizoi J, Shinozaki K, Yamaguchi-Shinozaki K. NAC transcription factors in plant abiotic stress responses. Biochim Biophys Acta. 2012; 1819: 97–103.
75. Vidal EA, Alvarez JM, Gutierrez RA. Nitrate regulation of AFB3 and NAC4 gene expression in Arabidopsis roots depends on NRT1.1 nitrate transport function. Plant Signal Behav. 2014; 9: e28501.
76. Love MI, Huber W, Anders S. Moderated estimation of fold change and dispersion for RNA-seq data with DESeq2. Genome biol. 2014; 15(12): 550

Figures

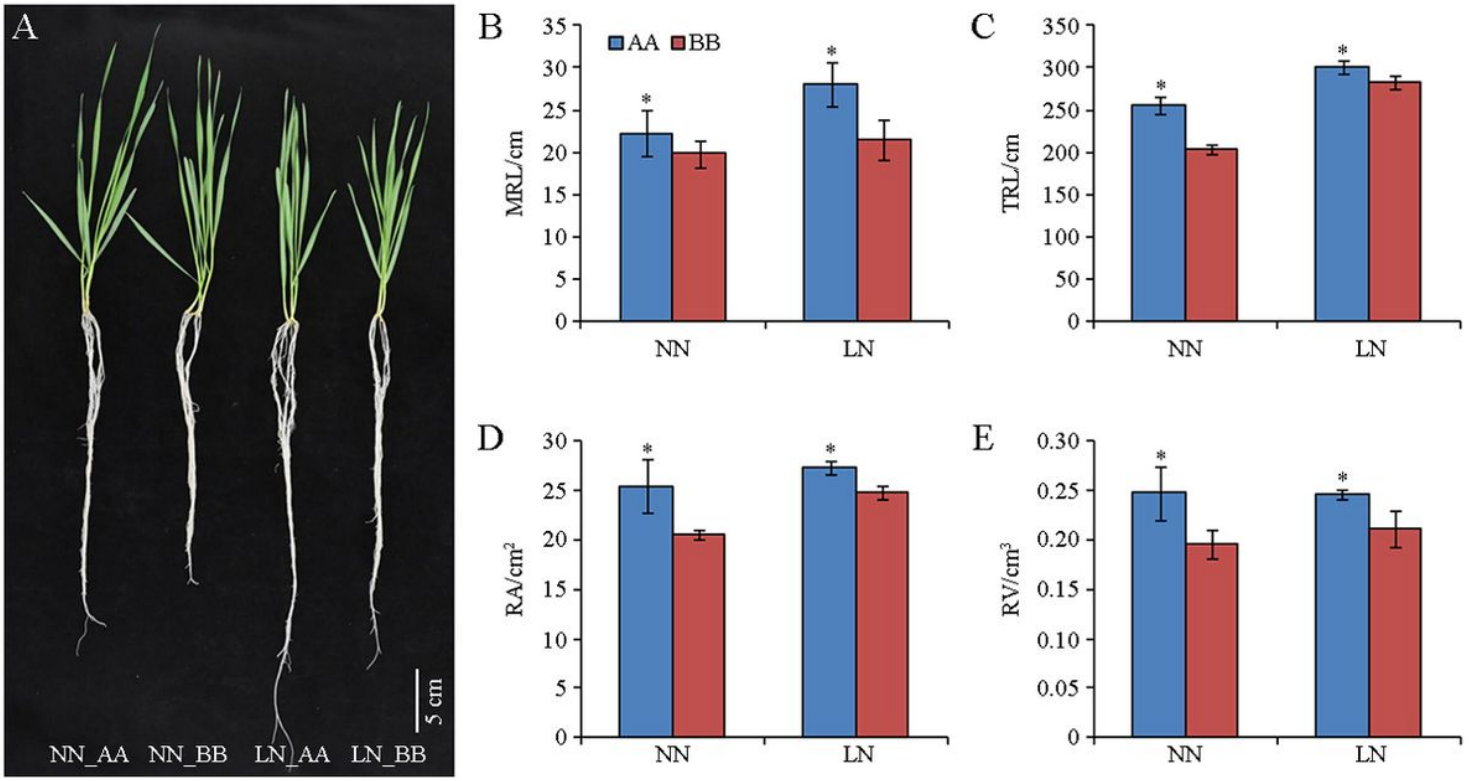

Figure 1

Phenotypes of four-leaf-stage seedlings (A) and the corresponding root traits (B-E) of the pairwise NILs cultured in nutrient solutions with different N contents for fourteen days NN and LN indicate normal- and low-nitrogen conditions, respectively. AA and BB indicate the A-NIL, which has superior alleles, and the B-NIL, which has inferior alleles, respectively. MRL, TRL, RA and RV indicate the maximum root length, total root length, root surface area and root volume, respectively. The "*" indicates a significant difference at $p < 0.05$.

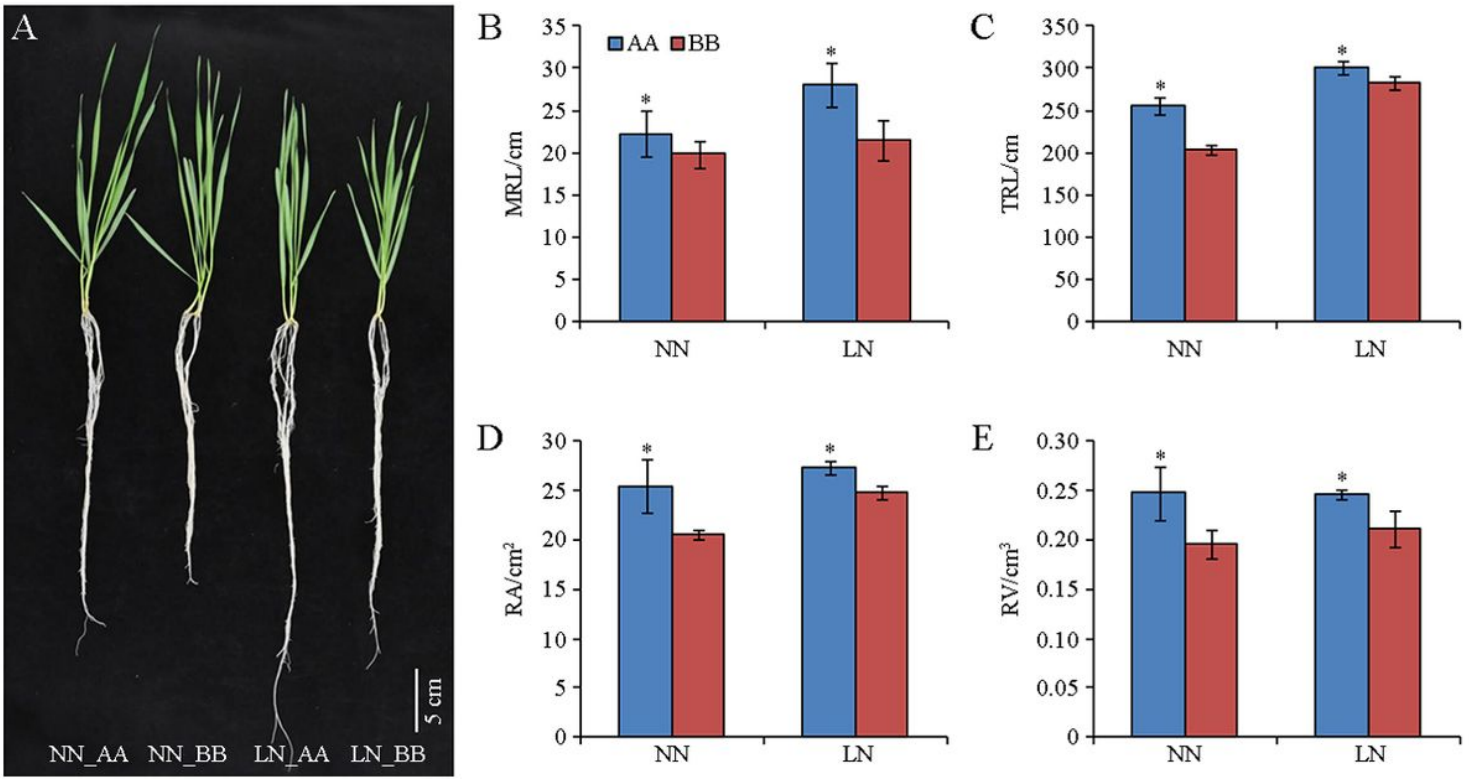

Figure 1

Phenotypes of four-leaf-stage seedlings (A) and the corresponding root traits (B-E) of the pairwise NILs cultured in nutrient solutions with different N contents for fourteen days NN and LN indicate normal- and low-nitrogen conditions, respectively. AA and BB indicate the A-NIL, which has superior alleles, and the B-NIL, which has inferior alleles, respectively. MRL, TRL, RA and RV indicate the maximum root length, total root length, root surface area and root volume, respectively. The “*” indicates a significant difference at $p < 0.05$.

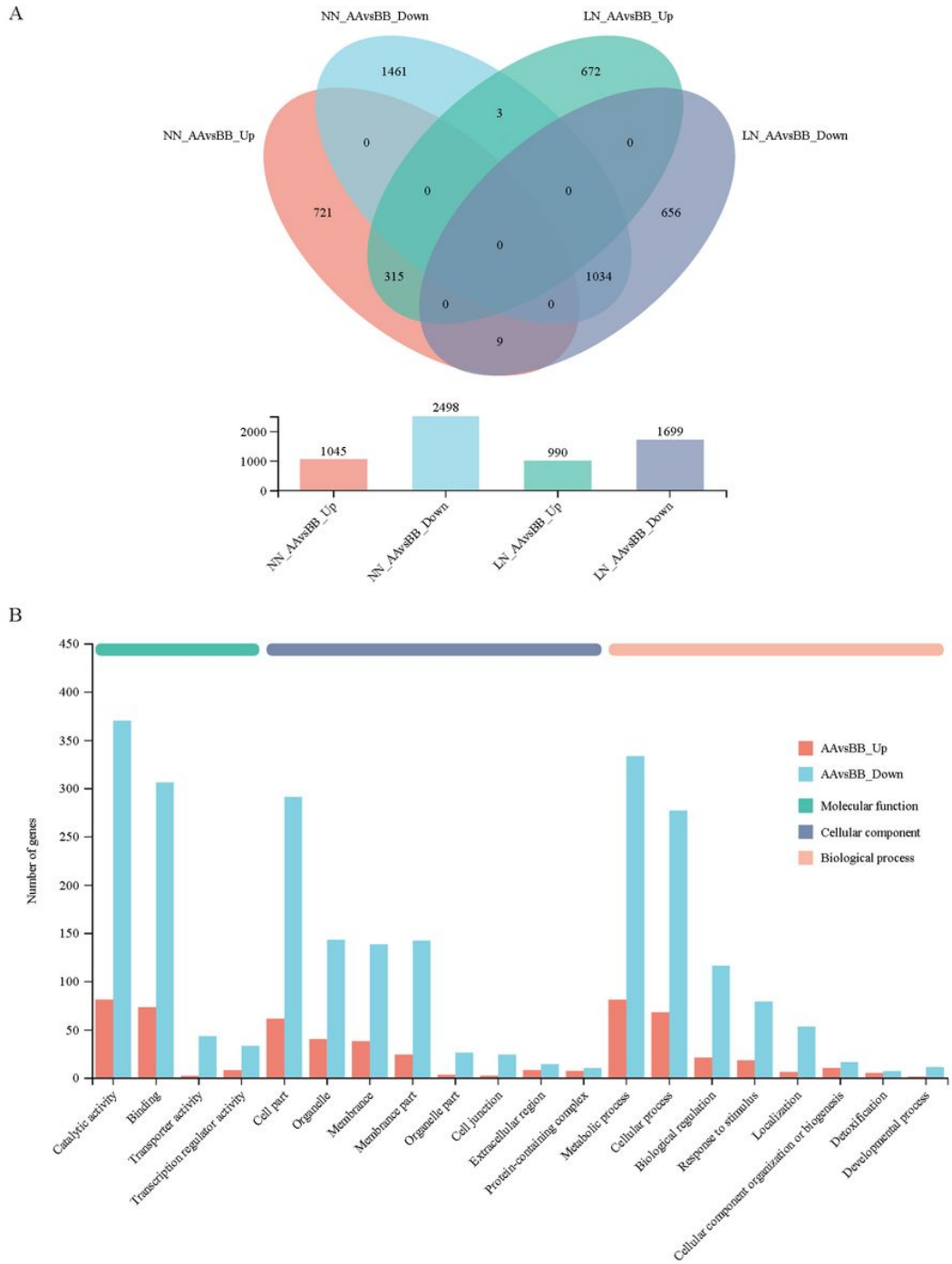

Figure 2

Identification of DEGs between the pairwise NILs NN and LN indicate normal- and low-nitrogen conditions, respectively. AA and BB indicate the A-NIL and the B-NIL, respectively. The expression levels between the A-NIL and

the B-NIL were compared under each condition, with the former as a control. BBvsAA_Up and BBvsAA_Down indicate DEGs whose expression was upregulated and downregulated in the B-NIL compared to the A-NIL under the same culture conditions, respectively. (A) Venn diagram analysis of DEGs in each one-to-one comparison between the pairwise NILs under both NN and LN conditions. (B) GO annotation analysis of DEGs between the pairwise NILs that were simultaneously expressed under both NN and LN conditions with the first 20 terms as indicated.

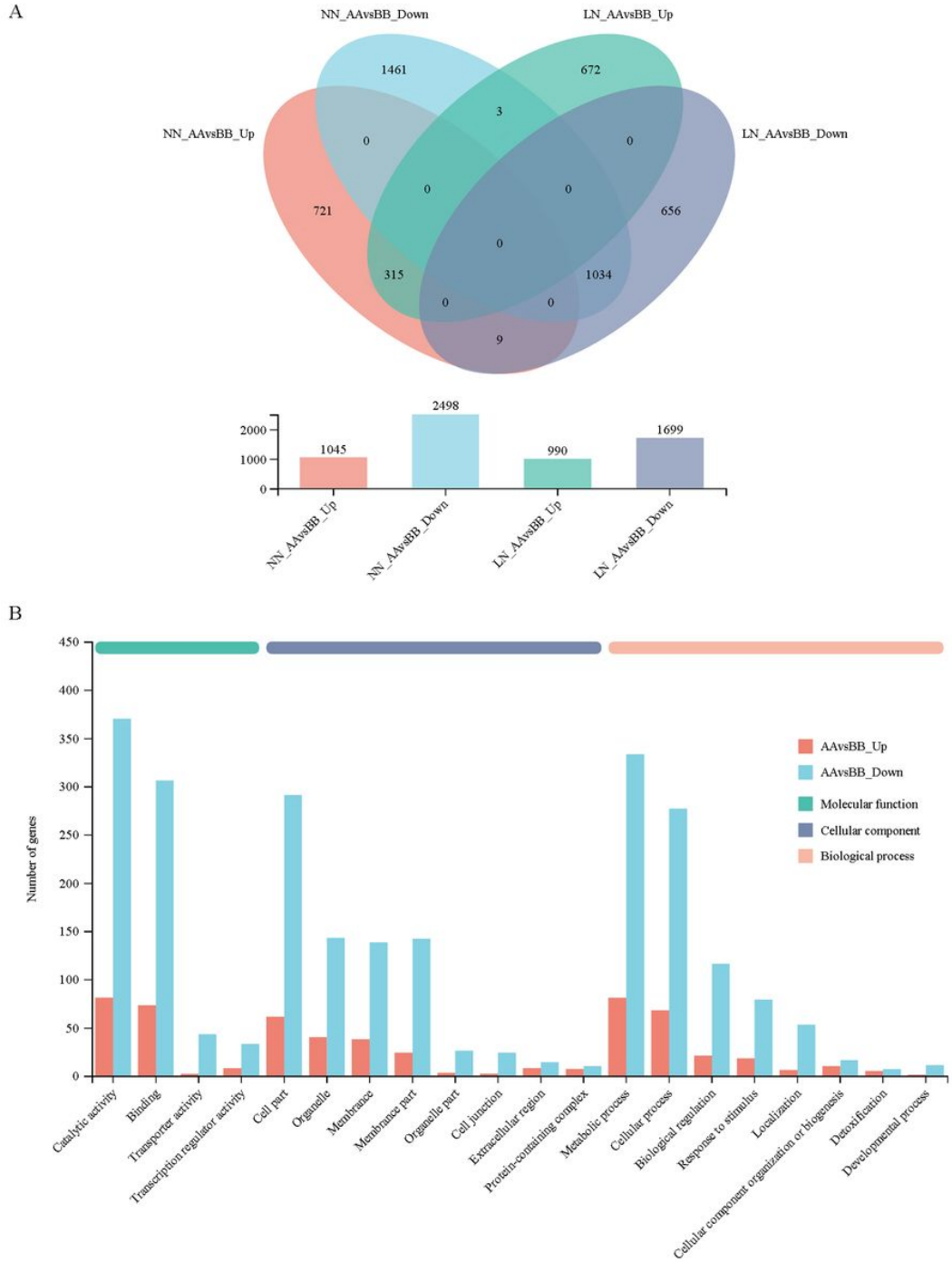

Figure 2

Identification of DEGs between the pairwise NILs NN and LN indicate normal- and low-nitrogen conditions, respectively. AA and BB indicate the A-NIL and the B-NIL, respectively. The expression levels between the A-NIL and the B-NIL were compared under each condition, with the former as a control. BBvsAA_Up and BBvsAA_Down indicate DEGs whose expression was upregulated and downregulated in the B-NIL compared to the A-NIL under the

same culture conditions, respectively. (A) Venn diagram analysis of DEGs in each one-to-one comparison between the pairwise NILs under both NN and LN conditions. (B) GO annotation analysis of DEGs between the pairwise NILs that were simultaneously expressed under both NN and LN conditions with the first 20 terms as indicated.

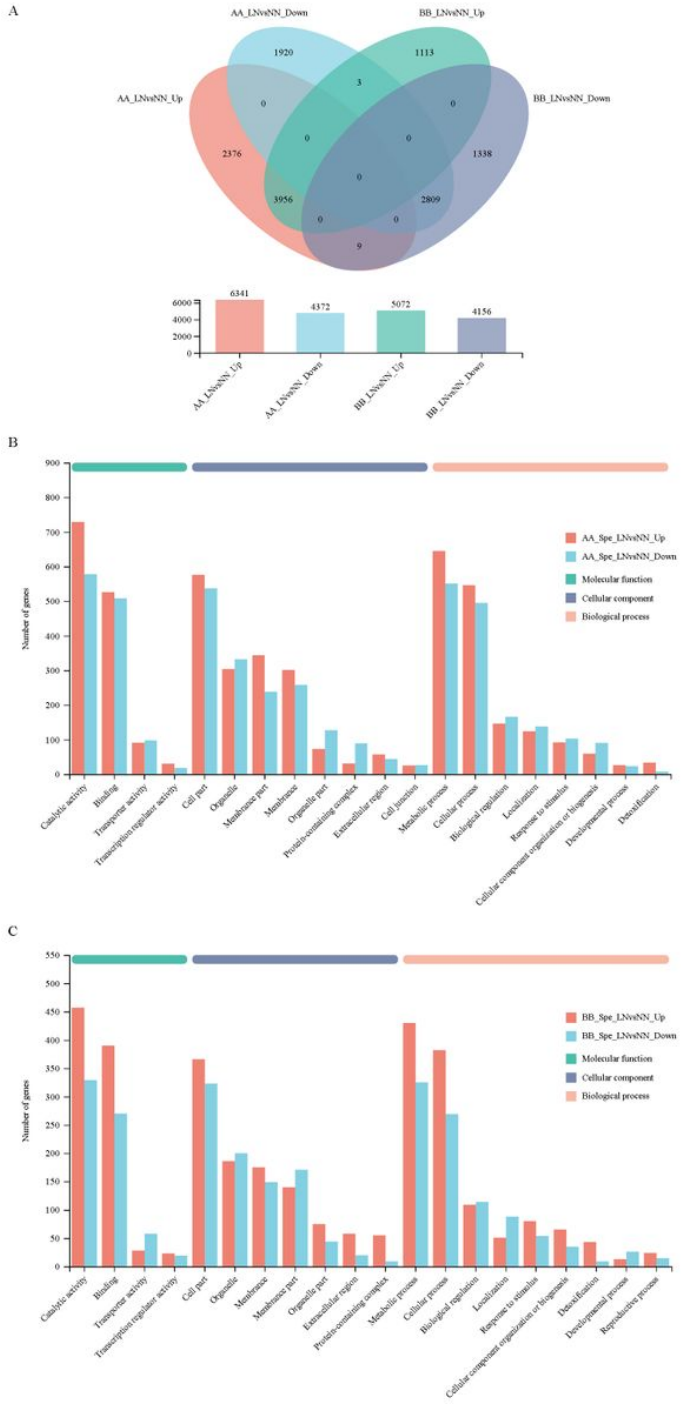

Figure 3

Identification of DEGs induced by LN NN and LN indicate normal- and low-nitrogen conditions, respectively. AA and BB indicate the A-NIL and the B-NIL, respectively. Spe indicates DEGs specifically expressed in the A-NIL or the B-NIL. The expression levels between NN and LN conditions were compared for each NIL, with the former as a control. LNvsNN_Up and LNvsNN_Down indicate DEGs whose expression was upregulated and downregulated under LN compared to NN for the same NIL. (A) Venn diagram analysis of the DEGs in each one-to-one comparison between

NN and LN conditions for both the A-NIL and B-NIL. (B-C) GO annotation analysis of the genes whose expression differed specifically in the A-NIL (B) and B-NIL (C) with the first 20 terms as indicated.

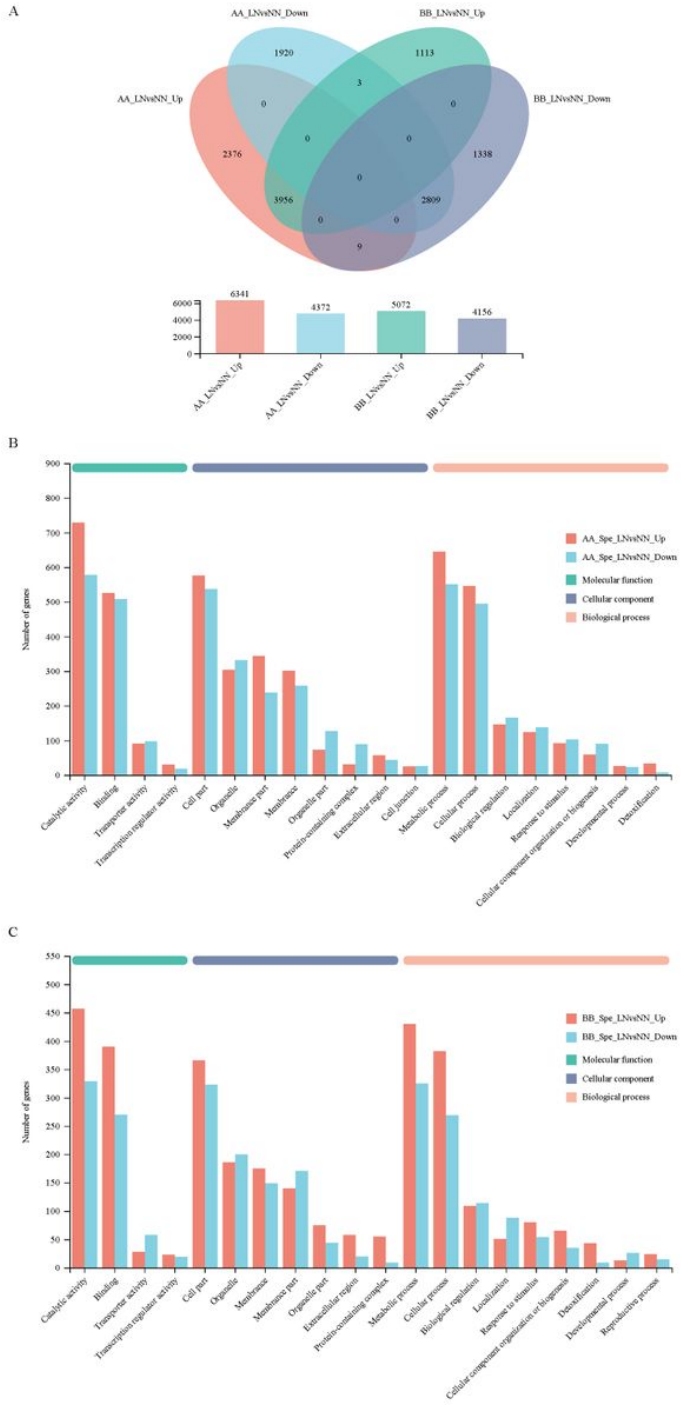

Figure 3

Identification of DEGs induced by LN NN and LN indicate normal- and low-nitrogen conditions, respectively. AA and BB indicate the A-NIL and the B-NIL, respectively. Spe indicates DEGs specifically expressed in the A-NIL or the B-NIL. The expression levels between NN and LN conditions were compared for each NIL, with the former as a control. LNvsNN_Up and LNvsNN_Down indicate DEGs whose expression was upregulated and downregulated under LN compared to NN for the same NIL. (A) Venn diagram analysis of the DEGs in each one-to-one comparison between NN and LN conditions for both the A-NIL and B-NIL. (B-C) GO annotation analysis of the genes whose expression differed specifically in the A-NIL (B) and B-NIL (C) with the first 20 terms as indicated.

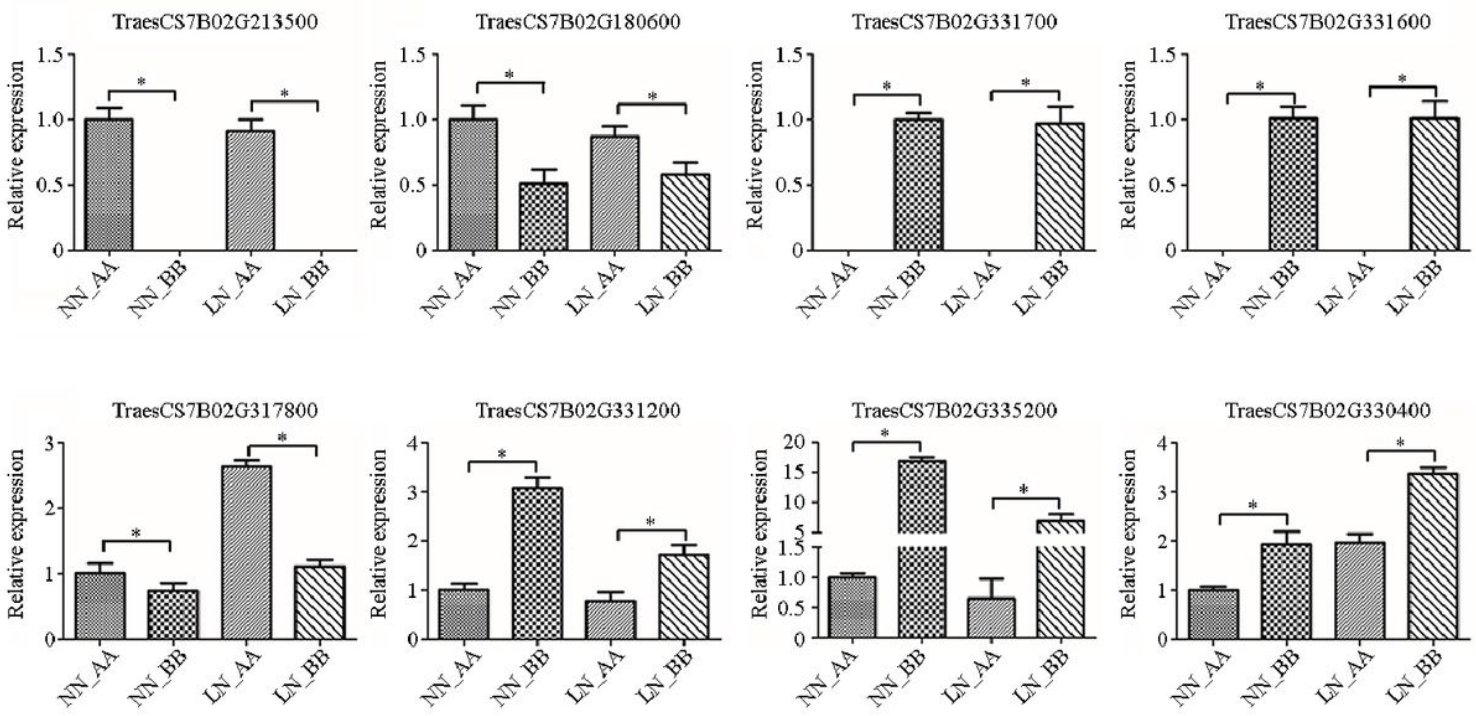

Figure 4

Validation of gene expression by qPCR The relative mRNA expression of 8 representative genes was checked by qPCR. Each bar shows the mean ± standard error of three biological replicates. The "*" indicates a significant difference at $p < 0.05$.

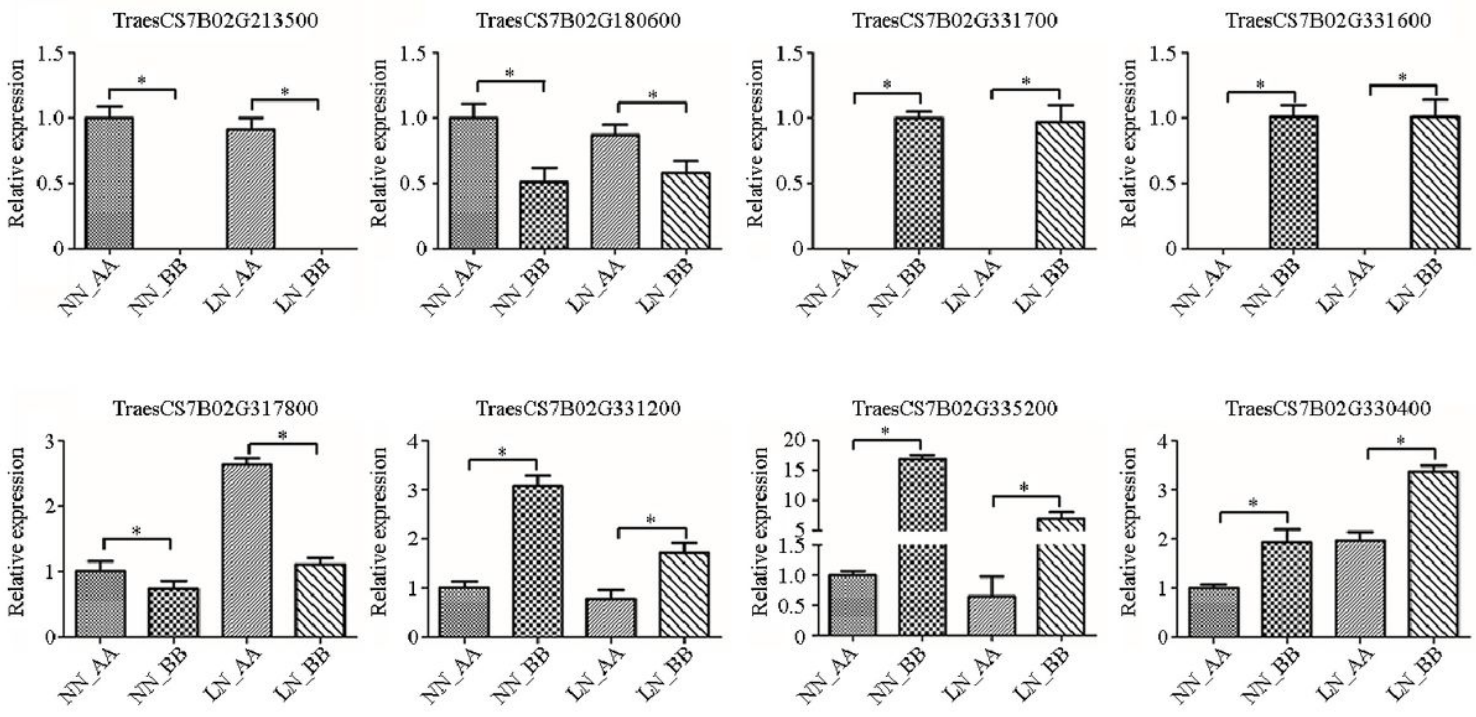

Figure 4

Validation of gene expression by qPCR The relative mRNA expression of 8 representative genes was checked by qPCR. Each bar shows the mean ± standard error of three biological replicates. The "*" indicates a significant difference at $p < 0.05$.

Supplementary Files

This is a list of supplementary files associated with this preprint. Click to download.

- supplementaryinformation.doc
- supplementaryinformation.doc
- SupplementaryFigure1.tif
- SupplementaryFigure1.tif
- SupplementaryFigure2.tif
- SupplementaryFigure2.tif
- supplementaryTablesS1S19.xlsx
- supplementaryTablesS1S19.xlsx